2021

AN APPROACH FOR PREDICTING FLOW CHARACTERISTICS AT THE CONTINUOUS MINER FACE

Kayla Henderson
University of Kentucky, knmayfield@live.com
Author ORCID Identifier:
https://orcid.org/0000-0002-0240-4450
Digital Object Identifier: https://doi.org/10.13023/etd.2021.391

STUDENT AGREEMENT:

I represent that my thesis or dissertation and abstract are my original work. Proper attribution has been given to all outside sources. I understand that I am solely responsible for obtaining any needed copyright permissions. I have obtained needed written permission statement(s) from the owner(s) of each third-party copyrighted matter to be included in my work, allowing electronic distribution (if such use is not permitted by the fair use doctrine) which will be submitted to UKnowledge as Additional File.

I hereby grant to The University of Kentucky and its agents the irrevocable, non-exclusive, and royalty-free license to archive and make accessible my work in whole or in part in all forms of media, now or hereafter known. I agree that the document mentioned above may be made available immediately for worldwide access unless an embargo applies.

I retain all other ownership rights to the copyright of my work. I also retain the right to use in future works (such as articles or books) all or part of my work. I understand that I am free to register the copyright to my work.

REVIEW, APPROVAL AND ACCEPTANCE

The document mentioned above has been reviewed and accepted by the student's advisor, on behalf of the advisory committee, and by the Director of Graduate Studies (DGS), on behalf of the program; we verify that this is the final, approved version of the student's thesis including all changes required by the advisory committee. The undersigned agree to abide by the statements above.

Kayla Henderson, Student

Dr. Steven Schafrik, Major Professor

Dr. Jhon Silva-Castro, Director of Graduate Studies

AN APPROACH FOR PREDICTING FLOW CHARACTERISTICS AT THE CONTINUOUS MINER FACE

DISSERTATION

A dissertation submitted in partial fulfillment of the
requirements for the degree of Doctor of Philosophy in the
College of Engineering
at the University of Kentucky

By
Kayla Mayfield Henderson
Lexington, Kentucky

Chair: Dr. Steven Schafrik, Professor of Mining Engineering
Lexington, Kentucky
2021

https://orcid.org/0000-0002-0240-4450

ABSTRACT OF DISSERTATION

An Approach for Predicting Flow Characteristics at the Continuous Miner Face

As coal and rock are mined, dust is dispersed into the air. This dust, among other contaminants, poses a serious health and safety risk to mineworkers. Very fine dust known as respirable dust can infiltrate the deepest part of the lungs, and long-term exposure to these particles leads to a disease called coal worker's pneumoconiosis (CWP). Occurrence of this disease declined steadily over the latter half of the 20th century; however, a recent study indicates that CWP has reemerged with an upward trend beginning at the turn of the century. To combat dust exposure, mine operators use a combination of water sprays and dust scrubbers in conjunction with face ventilation. Additionally, the University of Kentucky has developed a device that passively improves air infiltration to the coal face. Researchers use a variety of modeling techniques, including full-scale, reduced-scale, and computer modeling, to understand active-face flow phenomena. A one-twelfth scale model of an active continuous-miner face was constructed to examine airflow patterns under multiple conditions in a controlled environment. Fluid characteristics and boundary conditions have often been assumed in Computational Fluid Dynamics (CFD) models. Using particle-image-velocimetry (PIV), the flow patterns under various conditions can be measured. The results of these scale model experiments can be used to develop scaling laws which help validate numerical modeling and design of more accurate physical models.

This dissertation presents airflow measurements taken within a reduced-scale model at multiple depths of cut by a continuous miner (CM) while utilizing a machine-integrated scrubber (an active device), a passive wing regulator, and a combination of the two. For conditions where the scrubber is on, there are three power settings, 85%, 100%, and 115% of the curtain air quantity. The results of these experiments identify the relationship of the airflow during the cutting phase and help researchers narrow the number of simulations needed as new ventilation controls or schemes are developed. It also provides realistic baseline cases which can be used for further comparisons.

KEYWORDS: face ventilation, coal mine safety, particle image velocimetry, reduced-scale modeling

Kayla Mayfield Henderson

(Name of Student)

September 15, 2021

Date

AN APPROACH FOR PREDICTING FLOW CHARACTERISTICS AT THE CONTINUOUS MINER FACE

By
Kayla Mayfield Henderson

Dr. Steven Schafrik
Director of Dissertation

Dr. Jhon Silva-Castro
Director of Graduate Studies

September 15, 2021
Date

ACKNOWLEDGMENTS

I want to express my sincerest gratitude to my dissertation advisor, Dr. Steven Schafrik, for his advice and guidance with my research. I appreciate the immense amount of time and flexibility he provided to help me complete my work.

I am also grateful to Dr. Thomas Novak for guiding me throughout my graduate studies at the University of Kentucky. I really enjoyed the opportunities provided to me to work on unique projects and to teach classes in automation and control. I also want to acknowledge the guidance provided by Dr. Joseph Sottile during my fellowship with the Central Appalachian Regional Education Research Center (ERC). I am eternally grateful for the financial support provided by the ERC.

Dr. Wala was a pioneer of mine ventilation at the University of Kentucky and his work inspired much of my research. I really appreciate his helpfulness in the lab as I constructed my model. I am thankful for the input of Dr. Chad Wedding early on in my dissertation work.

Lastly, I want to acknowledge Dr. Ashish Kumar who started his graduate study journey with me and has been a great source of information and support. I am also thankful to Dr. Sampurna Arya, Adam Levy, Oscar Velasquez, Anand Kumar, and other graduate students for their support and encouragement.

I must also express my deepest thanks to my family and my husband, Michael, who have stood by me during this process. Brian and Laura Groff have also been great sources of encouragement and support.

I acknowledge the Alpha Foundation for the Improvement of Mine Safety and Health, Inc. (ALPHA FOUNDATION) for sponsoring the project AFC215-15 Improved Face Ventilation for Extending-Cut Continuous Mining Using a Wing Regulator and Scrubber Control System. The views, opinions and recommendations expressed herein are solely those of the author and do not imply any endorsement by the ALPHA FOUNDATION, its directors, and staff.

TABLE OF CONTENTS

LIST OF TABLES

LIST OF FIGURES

CHAPTER 1. INTRODUCTION

Dust and other air contaminants pose a serious risk to the health and safety of mineworkers. As the coal and other rock are fractured, mining machinery disperses dust into the air and releases methane trapped within the strata. Of the dust generated at the face, the most concerning for miner health is respirable dust. Respirable dust is recognized as particles less than 10 microns in diameter (WHO, 1999). Particles this small can travel past the body's natural defenses to the deepest parts of the gas-exchange region within the lungs where the body is unable to remove them. Continuous exposure to respirable dust leads to pneumoconiosis – a generic term for damage caused by dust inhalation. In the mining industry, the two main forms of pneumoconiosis are coal worker's pneumoconiosis (CWP), also known as black lung, and silicosis caused by exposure to coal dust and silica dust, respectively (McPherson, 1993a).

1.1 The Issue and its Background

During the 20th century, prevalence of CWP diminished; however, NIOSH found that there was an increase in the disease, beginning in the late 1990's (NIOSH, 2008). These findings sparked increased research and new legislation to reduce dust exposures of mine workers. Starting August 1, 2016, the dust standards for the concentration of respirable-dust exposure for mine workers was lowered from 2.0 mg/m^3 to 1.5 mg/m^3, provided the quartz content of the dust is below five percent (30CFR70.101). It is too soon to know the results of the new dust standard; but, because CWP prevalence rates have continued to increase, particularly for miners in the Central Appalachia region (Hall, Blackley, Halldin, & Laney, 2019), more needs to be done to ensure miner health.

1.2 Mine Ventilation Network

In room and pillar coal mine ventilation, fresh air enters the mine through either a shaft or adit. Airways, which may consist of multiple parallel entries, are primarily categorized into three types: intake, neutral, and return as shown in Figure 1.1. Fresh air is delivered to the working areas via the intake airway, and the contaminated air is exhausted through the return. The neutral is generally between the intake and return functioning as a buffer between them.

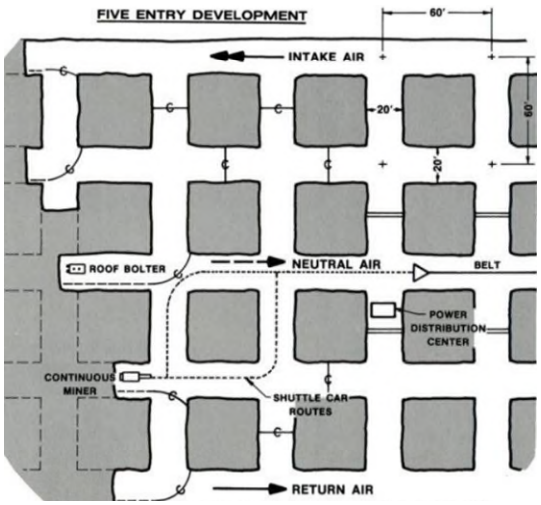

Figure 1.1 Ventilation of a Five Entry Section (Williams, 2005)

The minimum quantity of intake air needed to reach the working face is 3000 cubic feet per minute (cfm), as defined by regulations (30 CFD 75.325). However, in practice, this minimum is usually exceeded to dilute and remove dangerous and harmful gases.

During the ventilation system design, the airflow requirements, with losses, considered, are used to determine the required quantity and pressure of the main mine fan(s) used to ventilate the mine. The air produced by the mine fan is directed to each working section and controlled via the following passive devices: stoppings, regulators, airlocks, overcasts/undercasts, and line brattices.

1.2.1 Stoppings

In the room and pillar method of coal mining, coal is extracted by continuous miners that create a grid-like pattern of passageways through the coal seam. The forward extraction areas are the entries and can be a variety of lengths and widths depending on the roof control plan. These entries are connected to one another by crosscuts (also called breaks). This network forms pillars of coal, left in place to support the overhead rock, or roof. For ventilation control, air is directed through the entries and to prevent inappropriate mixing of air between passageways, miners use brattices called stoppings which can be masonry, block, or steel (Kennedy stoppings). Even well-maintained stoppings incur leakage across them (Oswald, Prosser, & Ruckman, 2008).

Because stoppings occur at each crosscut, the total loss can be quite significant. The presence of man doors (a small steel or wood door required at certain intervals for personnel to egress) also increases the leakage of a stopping.

1.2.2 Regulators

To control airflow at localized places or the splitting of air at a section, mines utilize a system of regulators. In principle, a regulator uses the difference in the airway resistance of parallel airways to control the air quantity and its direction. The intentional resistance of the regulator is usually created by establishing a shock loss by abruptly changing the dimensions of the airway by installing a curtain across the entry or installing a variable-size opening in a stopping.

1.2.3 Airlocks

Because airways serve a dual purpose of supplying air and providing passageways for equipment and personnel, an airlock is sometimes needed to create a neutral zone for passing from one airway type to another. The use of two doors decreases the pressure on the individual doors, making them easier to open with less contamination or loss that occurs with a single door.

1.2.4 Overcasts and Undercasts

Overcasts and undercasts are used to bridge air over and under, respectively, another airway while maintaining isolation between the airways. They can be made of block, masonry, or steel.

1.2.5 Line Brattices

Line brattices represent the last passive air control device used for controlling flow at the active face. A canvas curtain is suspended from the roof and offset from the rib as specified in the ventilation plan. This curtain directs intake air to the working face where mining occurs. Line brattice is also required in the other face entries where mining is not occurring to continuously dilute gas being liberated from newly exposed coal surfaces.

Figure 1.2 Example of brattice cloth installed in a heading.

1.2.6 Wing Regulator

A wing regulator is a ventilation control device that was developed at the University of Kentucky. The device addresses the problem of the intake air flowing directly from the end of the curtain to the exhaust. This is due to force of the incoming air not being sufficient to carry the intake air straight along the rib to the cutting face. The wing regulator is an air foil shaped device that creates an air stream which passively boosts the intake air velocity, directly it toward the cutting face.

Figure 1.3 Prototype of the wing regulator.

1.3 Inefficient Face Ventilation

As mentioned, mine ventilation is critical to reducing contaminants in the air and maintaining a healthy, safe working environment. The system's design is critical to this function. At many operations, the amount of air that reaches the mining faces, which are the dust and methane generating zones, is a relatively low percentage compared with that produced by the mine ventilation fan(s) perhaps around 50% (Bise, 1986). (This ratio is generally called the mine ventilation volumetric efficiency). This reduced air quantity is due to losses in the system via leakage at control devices, such as stoppings and overcasts. It is also due to poor application of curtains at the face. Therefore, to meet section air demands, mine operators typically oversize ventilation fans resulting in higher energy costs. While some leakage is expected and even designed into the system, the air volume "lost" before reaching critical areas of the mine, such as the face, is already wasted so what is received at the section must be used efficiently and effectively.

1.4 Provide Method for Testing New Ventilation Technology

As new ventilation devices and equipment are being developed, they will require extensive phases of testing to demonstrate their effectiveness. A new concept often begins with a rendering and a numerical or computational model, allowing for multiple iterations of adjustment at relatively low expense. Physical models, however, are still a vital component of testing.

This dissertation presents airflow measurements taken within a reduced-scale model at multiple cut depths by a continuous miner while utilizing a machine-integrated scrubber (an active device), a passive wing regulator, and a combination of the two. For conditions in which the scrubber is operating, three airflow settings are used - 85%, 100%, and 115% of the curtain air quantity. The results of these experiments identify the relationship of the airflow during the cutting phase and helps researchers narrow the number of simulations needed as new ventilation controls or schemes are developed. It also provides realistic baseline cases that can be used for further comparisons.

1.5 Limitations & Assumptions

In this study, certain assumptions had to be made. It is well known that water sprays reduce the amount of dust in the air by suppression. Water sprays were not simulated in the reduced scale model due to complexity and because of incompatibility. It was assumed that any reduction of dust from the air which is not immediately suppressed by water sprays is directly related to the quantity of air supplied. The quantity at the curtain is related to the quantity of air that reaches the face area. The curtain flow at reduced scale velocities was limited to either the capabilities of equipment already available in the laboratory or reasonably acquirable.

CHAPTER 2. LITERATURE REVIEW

There have been several studies conducted over the last several decades on the effectiveness of a machine-mounted dust scrubber for the removal of respirable dust and on its relationship with the face ventilation system.

The literature review begins with a discussion of flow separation phenomena and the research that has been conducted in understanding the airflow patterns at a coal mine face. From there, research turns to how scrubbers affect this pattern, whether positively or negatively, and how the scrubber ultimately impacts the effectiveness of ventilation.

2.1 Mine Ventilation Requirements

A ventilation system is designed to remove and dilute contaminants to acceptable exposure levels. Compared to a standard cut depth, extended-cut continuous miner sections are more difficult for ventilation systems to supply the face with fresh air. An extended-cut or deep cut is defined as when the continuous miner is allowed a cut depth exceeding 20 feet, and up to a maximum of 40 feet beyond the last row of roof bolts (Stricklin, 2012).

Extraction is divided into two cuts, the box cut and slab cut. The box cut is created as the continuous miner, which is narrower than the final entry width, mines forward. The portion of the coal left behind forms the slab as shown in Figure 2.1.

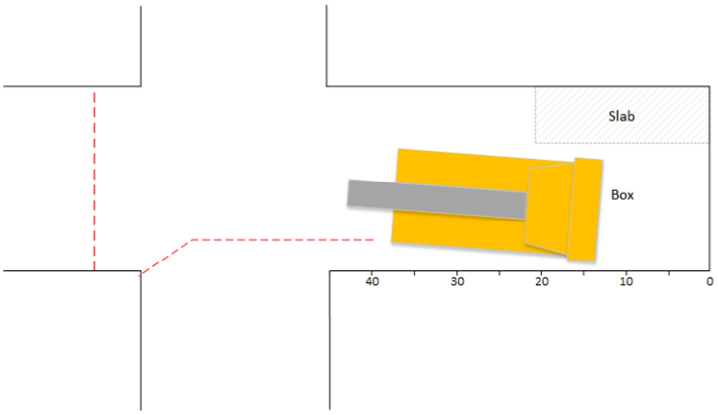

Figure 2.1 Continuous miner in the box cut area.

After the continuous miner completes this cut, it is reversed, and the remaining slab is mined as illustrated in Figure 2.2.

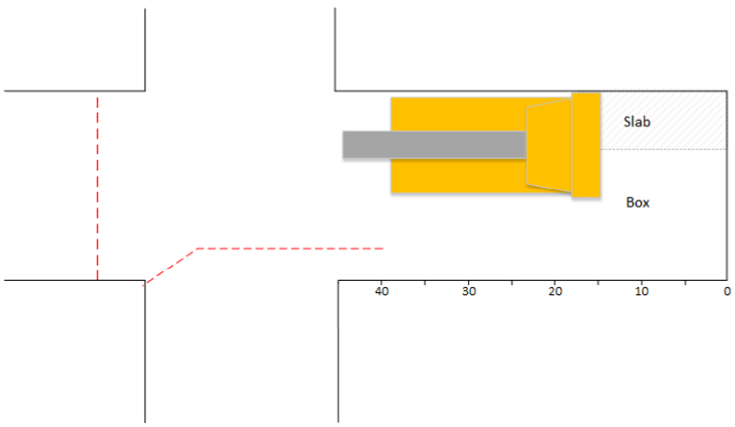

Figure 2.2 The continuous miner beginning to mine the slab.

Extended-cut mining requires the use of a remotely controlled continuous miner with a dust scrubber and accounts for the vast majority of all continuous miner sections. To meet Federal dust regulations, mine operators are required to utilize water sprays and machine-mounted dust scrubbers to suppress and remove airborne particles, respectively.

The scrubber system and the location of the continuous-miner operator play essential roles in reducing the exposure of the continuous miner operator to respirable dust.

The performance of a dust scrubber is measured by two characteristics: capture efficiency and cleaning efficiency. Capture efficiency is the percentage of total dust generated that is drawn into the scrubber, and cleaning efficiency is the percentage of the dust removed from the captured air (Wirch & Jankowski, 1991). However, the effectiveness of the scrubber in removing dust is largely dependent on both the airflow supplied to the face, as well as the airflow capacity of the scrubber. Capture efficiency optimization necessitates the study of this relationship and how parameters affecting the face airflow should be accounted for in selecting the scrubber air quantity.

Scrubber capacity is also related to the air quantity delivered to the face. Currently, MSHA recommends that the air quantity provided by the line curtain/brattice be equal or limited to 1,000 ft^3/min above the capacity of the scrubber. An air quantity above this limit is thought to overwhelm the scrubber and allow dusty air to evade the inlet (Schultz & Fields, 1999) particularly if a blowing ventilation system is utilized (Goodman, Taylor, Colinet, & Thimons, 2000). Recall that the minimum airflow required to ventilate the active face is 3,000 cubic feet per minute (30 CFR75.325); although, most coal mines operate above this minimum. However, studies have shown that a significant portion of the air supplied to the line brattice does not reach the face, especially with the deep cut technique (Colinet, Rider, Listak, Organiscak, & Wolfe, 2010).

2.2 Ventilation Schemes

Fresh air from the mine's ventilation network is directed to the face using a system of curtains, also known as line brattices. Curtains are installed temporarily in the entry and

are advanced after each cut with the distance from the face to the end of the curtain referred to as the setback. There are two standard face ventilation schemes: blowing and exhausting. The major apparent differences between a blowing and exhausting system is the direction of the air with respect to the curtain.

In the blowing system, illustrated in Figure 2.3, intake air is directed towards the face from behind the line brattice (called the tight side) and immediately splits at the end of the curtain with a significant portion flowing directly to the return airstream (Petrov, Wala, & Huang, 2013). The continuous miner operator is able to position him/herself in the intake air at the end of the curtain, but the secondary equipment operators (e.g. shuttle car operators) will always be located in the return airway (Colinet et al., 2010). This face ventilation arrangement confines the continuous miner operator to that designated area if he/she desires to stay within the fresh air supply. Thus, the blowing ventilation system reduces the operator's visibility by confining him/her to a specific location. It is considered, however, to be the most effective system for the removal of methane gas (Reed & Taylor, 2007).

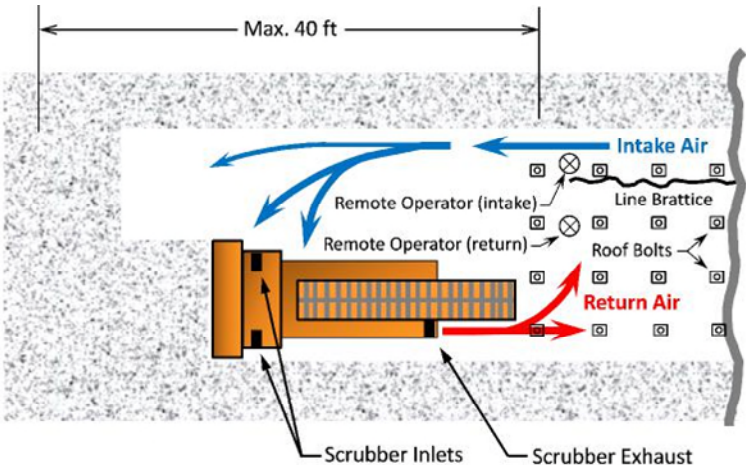

Figure 2.3 Blowing Ventilation System

In the exhausting system, intake air is delivered from the off-curtain, or wide, side. This method (shown in Figure 2.4) affords the best positions for the mineworkers as it provides a greater range of movement and visibility for the continuous miner operator and places other workers, e.g., shuttle car operators, in the intake air. For this reason, it is also the preferred method of MSHA for underground coal mines (Stricklin, 2012). The scrubber, however, must be turned off during a significant amount of time when using the exhaust system because the end of the line brattice must always be behind the scrubber discharge. Nonetheless, some researchers feel that the exhausting system has a performance advantage over the blowing system in terms of dust removal (Schultz & Fields, 1999), because the dust and contaminants are swept to the return side of the airways via the curtain or exhaust tubing.

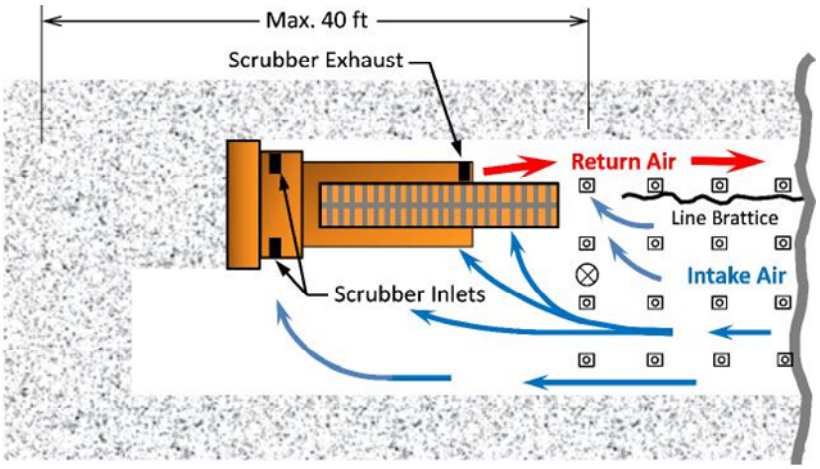

Figure 2.4 Exhausting Ventilation System

Both methods rely on fresh air reaching the face to dilute and sweep away the contaminants, and in each case, separation phenomenon occurs at the end of the curtain (Petrov et al., 2013). Dust scrubbers help fresh air to reach the face by pulling air toward the scrubber inlets. In fact, in blowing systems, the curtain airflow can increase significantly with the activation of the scrubber (Taylor, Rider, & Thimons, 1997). As expected, the curtain setback has also been found to significantly influence the face air pattern (Thimons, Taylor, & Zimmer, 1999).

2.3 Flow Separation Phenomena

It is a widely accepted fact in industry that the intake airstream separates shortly after passing the end of the line brattice. Determining the fraction of air that ventilates the face is difficult in practice but has been studied experimentally. Experimentation has found that as much as 80% of the air in a blowing system immediately joins the return stream leaving only 20% of fresh air to ventilate the face called the “secondary” flow (Petrov et al., 2013).

The nature of extended cuts offers an additional challenge to supplying fresh air to the face. It has been found that the geometry of the box cut and the line-curtain offset play a significant role in flow separation (A. Wala, Jacob, Brown, & Huang, 2003).

Using a combination of particle image velocimetry (PIV) and computational fluid dynamics (CFD), Petrov (2013) determined an empirical criterion (Eqn 2.1) called the Jet Separation Ratio (*JSR*).

$$JRS = \left(\frac{d'}{d}\right)^2 \tag{2.1}$$

where $d'$is the tight rib distance and d is the entry width minus the tight rib distance. If JSR > 0.02, then flow separation occurs regardless of intake air quantity.

NIOSH conducted full-scale experimentation to examine the secondary flow's ability to ventilate the face in a 40-ft box cut with a blowing system at different continuous miner positions. Without a dust scrubber and intake air flows of 10,000 and 4000 cfm, face air measurements were 538 cfm (5% of the available curtain air) and 552 cfm (14% of the available curtain air), respectively (Thimons et al., 1999). Researchers at NIOSH (Taylor, Chilton, Hall, & Timko, 2006) also concluded that, in a similar scenario, face air velocities were practically zero. These findings support the notion that increased curtain air alone does not supply enough air to ventilate the face, and further demonstrates the need for additional dust control methods like dust scrubbers.

2.4 How Scrubbers affect Face Ventilation

Flooded-bed dust scrubbers are incorporated into continuous miners as shown in Figure 2.5. The scrubber reduces dust concentration by drawing the dust-laden air from the

face through a wire-mesh panel that is continuously sprayed with water. At this point, dust is entrapped within the water droplets. The dirty water is removed from the air/water mist via the de-mister before the clean air is discharged. This type of scrubber is desirable for mining applications as maintenance is minimal compared to other wet scrubbers (McPherson, 1993b).

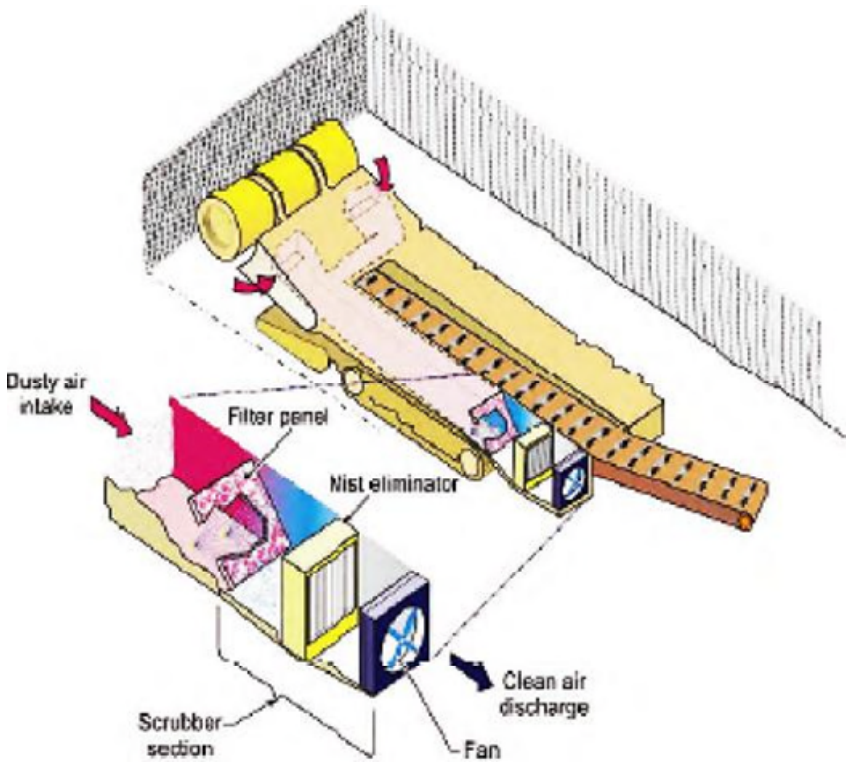

Figure 2.5 Components of a Flooded Bed Scrubber (Colinet et al., 2010)

A properly maintained flooded-bed dust scrubber has a high cleaning efficiency, but it also plays a significant role in the amount of air reaching the mining face. As previously discussed, it is difficult to force intake air to the face before leaving its forward trajectory and joining the return airstream. A scrubber helps to counteract this by drawing air directly up to the face area (Figure 2.6A). By increasing the turbulent flow at the front of a continuous miner, it also promotes better dilution of methane gas (Taylor et al., 1997).

Without the scrubber (Figure 2.6B), the face flow exhibits the typically seen “Figure Eight” pattern, whereby the fresh air separates and the secondary flow joins a recirculating zone near the front of the miner.

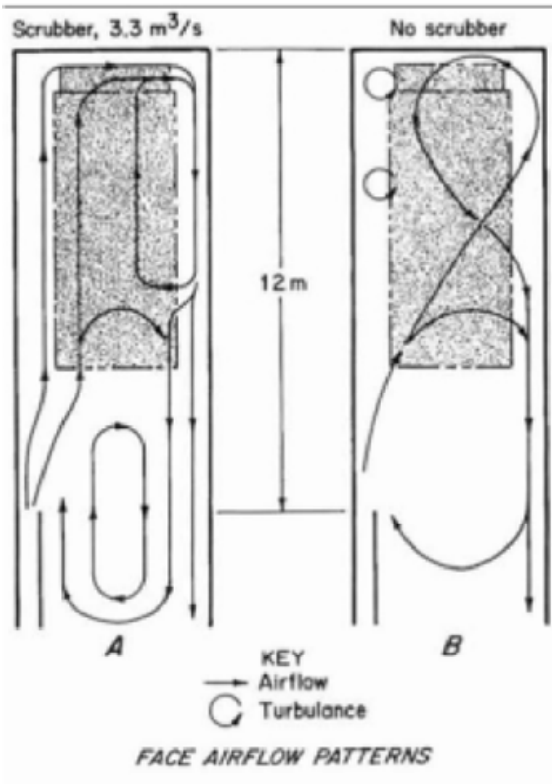

Figure 2.6 Face airflow pattern whereby the scrubber is on (A) and of (B) (Taylor et al., 1997).

The 40-ft box cut represents one of the most challenging ventilation scenarios of the extended cut method. In the Thimons, Taylor, and Zimmer (1999) study, scrubber operation improved face ventilation to approximately 50% of the available blowing curtain air for both 4000 and 10,000 cfm. Research at the University of Kentucky using PIV measurements of a scaled physical model and CFD analysis support the conclusion that, without the use of a dust scrubber, the blowing system was ineffective at ventilating the face (A. M. Wala, Jacob, Huang, Brown, & Rangubhotla, 2004). Thimons, Taylor, and

Zimmer also performed their tests for the slab cut. Sampling locations for their experiments are shown in Figure 2.7.

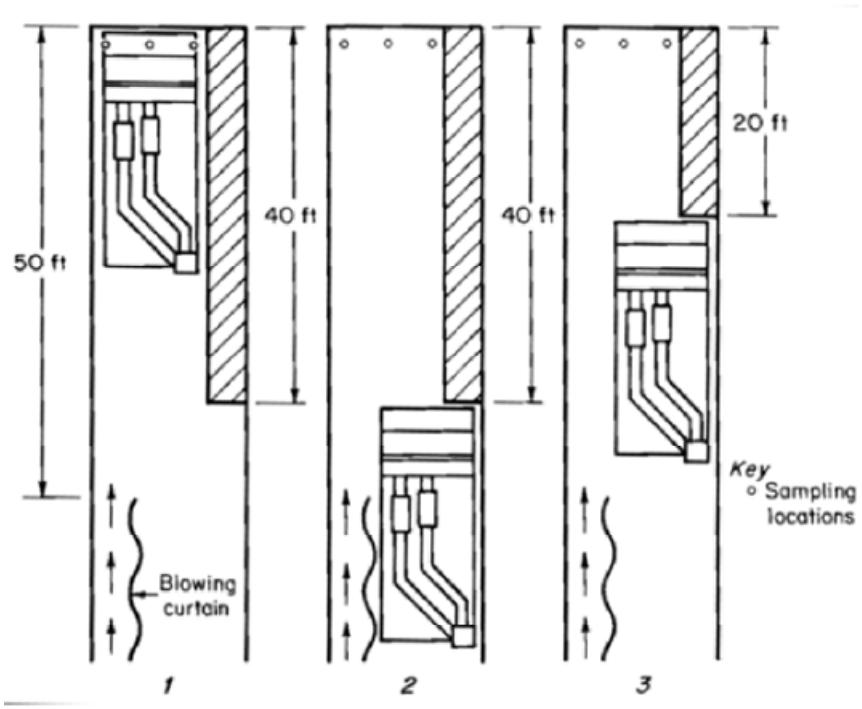

Figure 2.7 Sampling locations for the continuous miner extended cut sequence with 50 ft setback (Thimons et al., 1999).

During these tests, the researchers found that the higher intake (10,000 CFM) airflow rate was more effective at ventilating step 1 and 3 but had little advantage at step 2. The operation of the scrubber, which was operated at a one-to-one ratio to the curtain air quantity, had no significant impact on the air reaching the face when the continuous miner was at the start of the 40-ft slab cut (step 2). In the second round of testing, they tested the effects of various curtain setback distances for the blowing system. The results indicated that the curtains setback distance had a much greater impact on the airflow reaching the face than parameters in the first series.

2.4.1 The Ratio between Intake and Scrubber Airflow

The long-standing standard for scrubber operation is to establish an intake air quantity equal to the measured scrubber capacity and maintain them within 1000 cfm of each other. The idea being that intake air quantities greater than the scrubber air quantities can overwhelm the scrubber inlets, allowing dust to bypass them. In addition, it is believed that scrubber airflows greater than the intake airflows could lead to recirculation of air. While recirculation of air is not inherently bad, there has been a concern that it could allow methane to accumulate.

Taylor, Rider, and Thimons (1997) conducted a study of the relationship between the intake airflow and the capacity rating of the scrubber with respect to methane concentration at the working face of a continuous miner section. The study was conducted in a full-scale test gallery at the NIOSH Pittsburgh Research Center. Figure 2.8 is an illustration of their Methane Test Gallery. The test area was setup with a blowing face ventilation system.

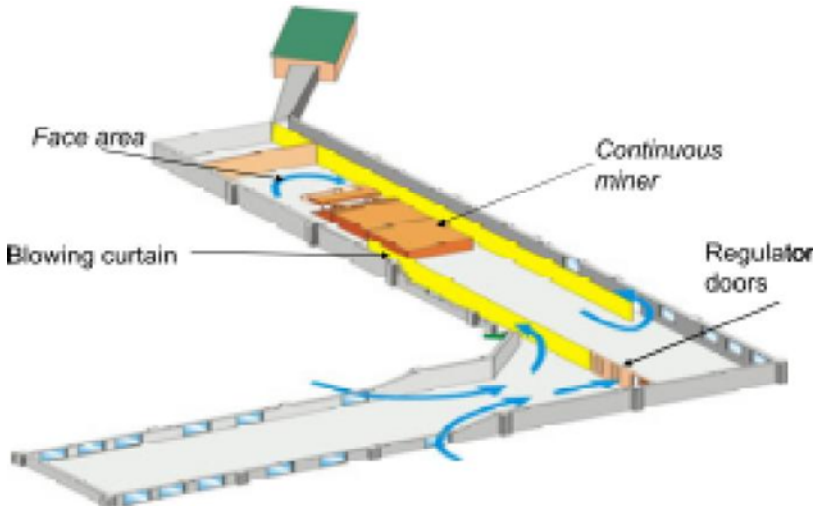

Figure 2.8 NIOSH Pittsburgh Research Center's Methane Test Gallery (A. M. Wala, Vytla, Taylor, & Huang, 2007)

Two fans were attached to the scrubber ductwork to operate at three airflows: 6000, which only required one fan to be energized, and 10,000 and 14,000 cfm, which required the operation of two fans. Airflow was controlled using orifice plates. The flow at the end of the brattice curtain was measured using a vane anemometer. The tests performed found that, as the scrubber flow increased, there was a decrease in the average concentration of methane. Results also revealed that an intake airflow less than that of the scrubber did not increase the methane levels as expected. This is likely because the scrubber increased the velocity of the intake air creating greater turbulence. In fact, the experiments showed that the operation of the scrubber created a significant effect on the velocity of the intake air.

2.4.2 Examining Recirculation

Goodman and Taylor (1993) developed a technique for determining the fraction of air being recirculated by the scrubber. The authors examined recirculation in a blowing face ventilation system with specific emphasis on extended-cut continuous miner sections.

In addition to evaluating the effect of setback distance and scrubber flow on recirculation, the researchers measured concentrations with and without a 30-ft long rigid duct attached to the scrubber outlet. A series of regression analyses were conducted based on the data collected during tests resulting in the following formulas:

For End-of-Box Cut,

$$r = 0.38367 - (0.03718)X_1 + (0.00513)X_2 - (0.13310)X_3 \qquad (2.2)$$

For End-of-Slab Cut,

$$r = 0.66306 - (0.01375)X_1 + (0.01041)X_2 - (0.46502)X_3 \qquad (2.3)$$

where, r is the scrubber re-circulation fraction, $X_1$is the curtain airflow minus scrubber airflow (m^3/s), X_2 is the setback distance (m), and X_3 is the tubing on scrubber (1 for yes, 0 for no).

The studies demonstrated the effect of the independent variables' influences on the resulting recirculation. For instance, the exhaust tubing had the greatest impact on recirculation reduction at the end of the slab-cut.

2.4.3 Respirable Dust Capture

Most coal mines in the US utilize flooded-bed dust scrubbers which are integrated into the continuous mining machine. Research has shown that these scrubbers can remove greater than 90% of the respirable dust captured on a mass basis (Colinet, McClelland, Erhard, & Jankowski, 1990). They are required as part of an approved ventilation plan for the extended (deep) cut.

In an evaluation of a dust scrubber's effectiveness in a 20-ft cut with an extended curtain setback, NIOSH (Colinet, Reed, & Potts, 2013) examined three underground coal mines anonymously named A, B, and C. The researchers measured the face and scrubber airflows at each operation and found that they met or exceeded the minimums specified by each mine's ventilation plan. Respirable dust measurements were taken using the following equipment: Personal Data Rams (pDRs); Personal Dust Monitor (PDM); and gravimetric samplers. The testing results showed that the dust scrubbers reduced dust concentration by 40% in the return air. However, there was insignificant difference in dust concentration for the CM operator at a maximum reduction of only 0.09 mg/m^3. This was likely due to the operations using exhausting face ventilation whereby the continuous miner operator could stay in intake air while moving around. The intake dust concentrations to the continuous miner faces were well below the dust standard for all three mines. An interesting takeaway from the studies found that Mine B and Mine C had an average reduction of 29% and 35% of scrubber airflow after each cut, respectively. This reduction was due to clogging in the flooded-bed screen and was resolved by cleaning the screen after each cut as part of the maintenance recommendation by NIOSH (Potts, Reed, & Colinet, 2011).

CHAPTER 3. METHODOLOGY

3.1 Introduction

This chapter describes the methodology used in the development of the reduced-scale model and the resulting analysis. This process started with field testing in active mine sites so that a full-scale model of the continuous miner face could be completed. This model was then developed into a reduced scale model of the face and continuous miner machine. The reduced scale model was necessary for particle image velocimetry (PIV) testing which could be correlated to the full-scale model and explanatory for active mine faces.

3.2 Field Testing

Surveys were conducted at three active coal mines within the United States, which will be referred to as Mines 1, 2, and 3. At each mine, a face area was set up by mine personnel for the tests in a manner typical of their operation. These mines all utilize a blowing ventilation scheme with a 40-ft setback for Mine 1 (as shown in Figure 3.1) and Mine 2, and a 45-ft setback for Mine 3. Because experimentation was performed with minimal impact to the production and operation of the mines, Mine 3 was the only mine for which a continuous miner was also available as part of the test.

The curtain was hung from the mine roof from roof bolts and secured with tension rods. Working within safety constraints and availability of mine personnel and supplies, deviations in the setback distances were made and noted. With the curtain set up, flags were attached evenly distributed to roof bolts in the entry to visualize the airflow. Air quantity behind the curtain (five feet from the setback) was measured at the beginning of each test for a total of three measurements to be averaged. The entry height and width

were measured. A TSI 9535 velocity meter was used to measure the airflow along the ribs taken at approximately two feet from each rib at five-foot spacing from the curtain to the face (or as close to the face as could safety be taken). Measurements made in Mine 1 are shown in Figure 3.1.

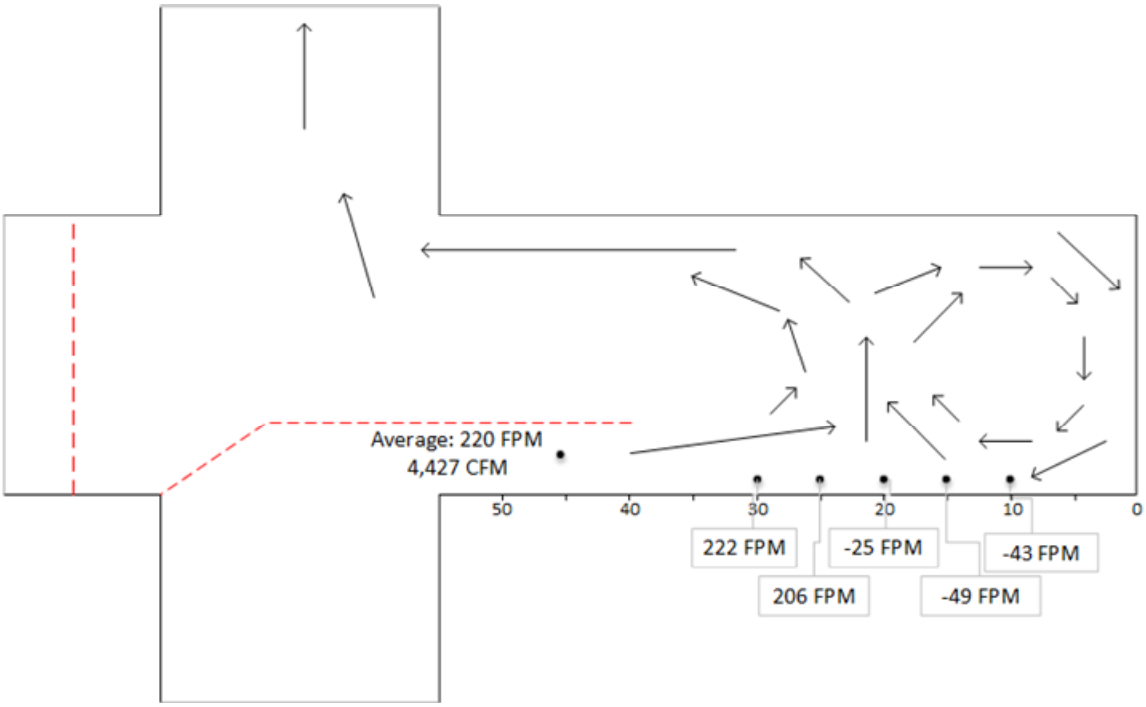

Figure 3.1. Field data collected at the Mine 1. (Schafrik, 2019)

In Figure 3.1, the black arrows are indications of flow recorded by the observer and are adapted from the source. Velocity readings, in feet per minute, are shown at the corresponding measurement point. Data collected for the other two mines are shown in the next chapter (Figure 4.2and Figure 4.1) in the same format. Mine 1 is typical of Central Appalachian mine and was chosen as the primary source for the models.

3.3 Full-Scale Model Development

The full-scale model, or dust gallery, was constructed at an underground limestone quarry in Georgetown, KY. The simulated coal face and crosscuts are 20-ft wide with a room height of seven feet. Figure 3.2 illustrates the design of the full-scale model. The gallery is a steel building on a concrete slab inside the mine with sealed corrugated plastic sheets. Parts of the walls are covered with roofing material to increase the surface roughness. Intake air is pulled from over a large mine sump area by an exhausting fan. The exhaust is blown over the sump around the corner from the intake with a large pillar separating the flow to prevent recirculation. A full-scale model of a continuous miner was constructed and is located within the gallery. Attachments points for repeatable and consistent ventilation control placement are available. The figure shows arrows for the typical direction of airflow.

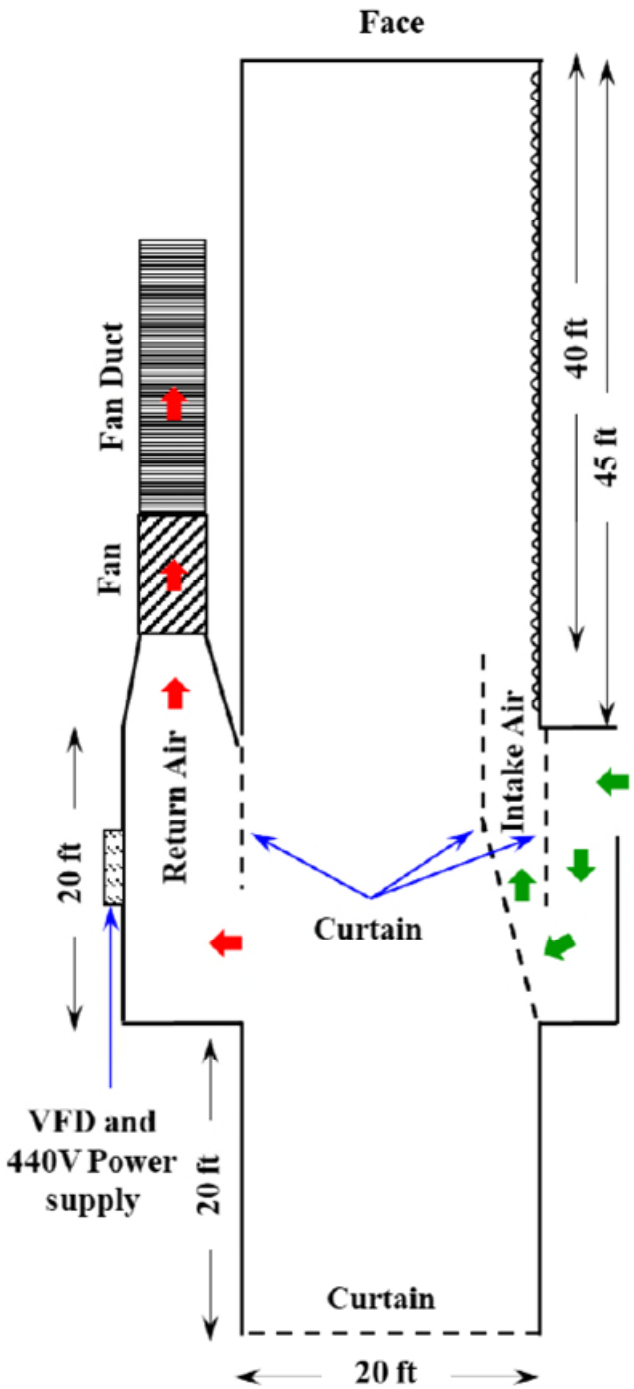

Figure 3.2 Schematic of the full-scale model, the Dust Gallery (Schafrik, 2019)

The continuous miner and main fan are supplied with 440VAC and are controlled by a central control center attached to the continuous miner model shown in Figure 3.3. The control center includes a Human Machine Interface (HMI) to allow researchers to easily control the fan speeds and cutter head rotation. The control elements are shown in Figure 3.4. The operational features of the continuous miner model include the following:

- Rotating cutter head
- VFD controlled scrubber
- Water sprays
- Control system for main fan, scrubber fan, and cutter head rotation.

Figure 3.3 Full-scale continuous miner model featured in front of the dust gallery. The PLC control center and scrubber VFD shown in the opening to the left.

Figure 3.4 HMI screen (top left) is connected to the PLC (bottom left) which is housed inside the CM model. It is used to control the main fan VFD, scrubber fan VFD (right), and Start/Stop of cutterhead rotation.

3.4 Reduced Scale Modelling

Researchers often employ scale models as a means for studying systems. Scale models are meant to accomplish three objectives:

- They allow researchers to work within manageable proportions of certain features of original phenomena that are difficult to handle, such as extreme size, very slow flow, vast energy release, and microscopic dimensions;
- They shorten experimentation by reducing the number of variables; and
- They promote a deeper understanding of the phenomena.

The following forces act in a moving fluid: inertial force, viscous force, gravitational force, pressure force, surface tension force, and elastic force. When modeling fluid flow in another scale, the model must account for viscous, gravitational, and inertial forces. These forces are given in Equations 3.1, 3.2, and 3.3.

Inertial forces, F_i

$$F_i = \rho L^2 u^2 \tag{3.1}$$

Gravitational forces, F_g

$$F_g = \rho L^3 g \tag{3.2}$$

Viscous forces, F_v

$$F_v = \mu L u \tag{3.3}$$

where, ρ is the density (kg/m^3), L is the characteristic length (m), u is the average velocity of the fluid (m/s), g is the acceleration of gravity (m/s^2), and μ is dynamic viscosity (N s/m^2).

Pi-numbers (π) are dimensionless numbers that have physical meaning. The ratio of these forces creates two important pi-numbers used in this research, Reynolds number and Froude number. The Reynolds number (3.4) deals with the relationship between viscous and inertial forces while Froude (3.5) deals with the relationship between gravitational and inertial forces.

$$\pi_1 = Re = \frac{F_i}{F_v} = \frac{\rho}{\mu} uL \tag{3.4}$$

$$\pi_2 = Fr = \frac{F_i}{F_g} = \frac{v}{\sqrt{lg}} \tag{3.5}$$

where π stands for pi-number. Flow is considered turbulent when Reynold's number is greater than 4,000. This was a strong consideration in choosing a velocity for testing in the reduced-scale model as it is well established that the airflow in the mine environment is turbulent. Therefore, only air velocities that remained in the turbulent range were considered for testing. This was particularly important for simulating the eddies that form adjacent to the face (Kumar, Henderson, & Schafrik, 2021).

Scaling laws can be described as: $\pi_i = \pi_i'$. For Reynold's number scaling (Eqn. 3.6), the resulting velocity is inversely proportional to the scaling ratio:

$$v' = \frac{l}{l'} v \tag{3.6}$$

where l is the full-scale characteristic length (i.e. hydraulic diameter) and l' is the equivalent characteristic length of the model.

For Froude number scaling (Eqn. 3.7), the velocity is inversely proportional to the square root of the scaling ratio:

$$v' = \frac{v}{\sqrt{\frac{l}{l'}}} \tag{3.7}$$

The hydraulic diameter of the tight side was used as the characteristic length for determining the scaled velocity. It is calculated by Equation 3.8.

$$D_h = 4\frac{A}{S} \tag{3.8}$$

where A is the cross-sectional area and S is the perimeter of the airway. The line brattice is offset by four feet from the rib in a seven-foot tall room. Therefore, the hydraulic diameter is 5.09 feet.

Using these principles, a set of full-scale curtain quantities was evaluated for use in the reduced-scale model. For instance, the air velocity (v') needed by the 1/12th scale model (therefore, $\frac{l}{l'}$ is 12) to model the full-scale intake airflow of 10,000 CFM is calculated where

$$v = \frac{10{,}000\ CFM}{4\ ft\ x\ 7\ ft} = 357\ fpm = 1.82\ m/s$$

using Reynolds pi-number as

$$v' = 12 * 357\ fpm = 4{,}286\ fpm = 21.79\ m/s$$

and using Froude pi-number as

$$v' = \frac{357\ fpm}{\sqrt{12}} = 103\ fpm = 0.52\ m/s$$

These calculations for multiple practical curtain quantities are summarized in Table 3.1.

Table 3.1 Calculations of reduced scale velocities for a practical of curtain quantities

			Reynold's Number Scaling		Froude Number Scaling	
Full-Scale Quantity	Full-Scale Curtain Velocity	Calculated Reynold's number	Reduced-Scale Curtain Velocity		Reduced-Scale Curtain Velocity	Calculated Reynold's Number
CFM	m/s		m/s		m/s	
5,000	0.91	95531	10.89		0.26	2298
6,000	1.09	114637	13.07		0.31	2758
7,000	1.27	133743	15.25		0.37	3217
8,000	1.45	152849	17.43		0.42	3677
9,000	1.63	171955	19.61		0.47	4137
10,000	1.82	191061	21.79		0.52	4596
11,000	2.00	210168	23.96		0.58	5056
12,000	2.18	229274	26.14		0.63	5515
*Curtain is a 4' by 7' X-Section at Full Scale ** Scaled Model is 1:12 ratio to the UK Dust Gallery						

3.5 Model Design

The laboratory model of the working place was constructed as a 1/12th scale model of the underground dust gallery described in 3.3. The model was developed as a way of determining airflow patterns for an extended cut. To facilitate PIV testing, the model must be designed with transparent walls and roof.

The 1/12th scale dust gallery was developed in CAD (see Figure 3.5) to facilitate its design and construction. The walls/ribs are assembled from flat pieces of 6mm thick acrylic that were precisely laser cut. Acrylic was chosen for its very high light transmissivity, affordability, and ease of construction. The base of the model is formed by two large black acrylic pieces. This base is supported by 2 in. x 4 in. dimensional lumber. The support creates a chase way for tubing to be run under the model and for the faux floor.

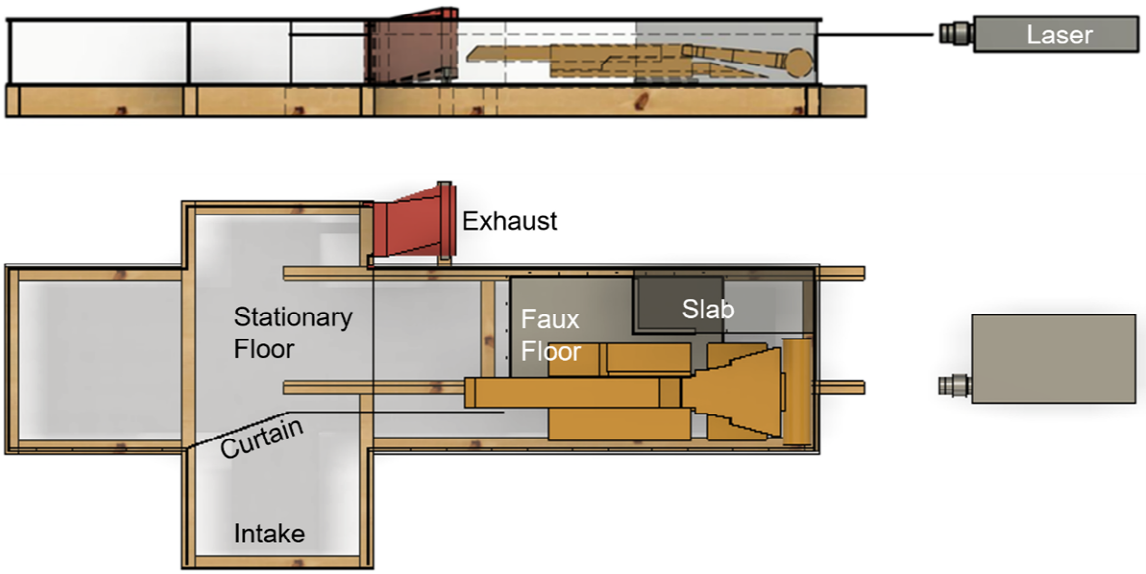

Figure 3.5 3D Render of 1/12th Scale Model

This faux floor, shown in Figure 3.6 in blue, was added to the model after initial testing. The faux floor system was added to provide a means of moving the miner and air tubing through the reduced-scale working place. This increased the ability for data collection of the airflow patterns with the miner in different positions without opening the model and permitted the transmission of “scrubber” air with minimal intrusion of the interior space.

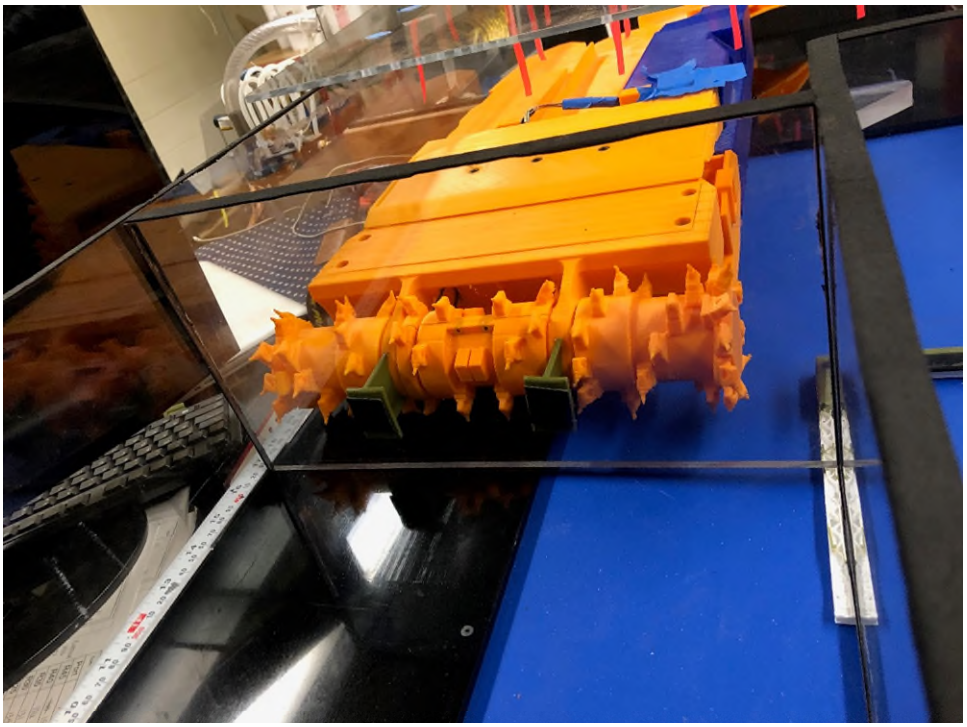

Figure 3.6 Faux coal face moves with the continuous miner; faux floor in blue.

3.5.1 Continuous Miner Model

The reduced-scale continuous miner model, as shown in Figure 3.7, was developed using computer modeling and 3D printing. The model was built modularly at 1/12th scale. Its features include the following:

- A coal discharge conveyor that can be manually raised and swiveled,
- A motor-controlled rotating cutter head that can be manually raised and lowered, and
- Scrubber model which allows air to be extracted and reintroduced to the model.

Figure 3.7 The 3D printed 1/12th scale model of the continuous miner.

The construction of the continuous miner model is modular. The scrubber module is featured in blue. Figure 3.8 illustrates the design of the scrubber module. The ducting, outlined in blue, was designed to be inherently printed within the part. A system of two vacuum cleaners was used to simulate the scrubber. Dust laden air, simulated by an oil mist, is sucked into a vacuum cleaner fitted with a filter to remove the oil droplets. A secondary vacuum, featuring a blower attachment, was attached to the exhaust side of the scrubber. Therefore, the exhaust only introduced clean air from the lab. The air quantity reintroduced via the "exhaust" was measured via a hotwire anemometer as it left the CM model. This was measured and adjusted to match the calculated scaled velocity for the scrubber airflow. Note that the purpose of the scrubber for these tests was to model the impact of the scrubber airflow on the airflow in the working place, not evaluate scrubber cleaning efficiency.

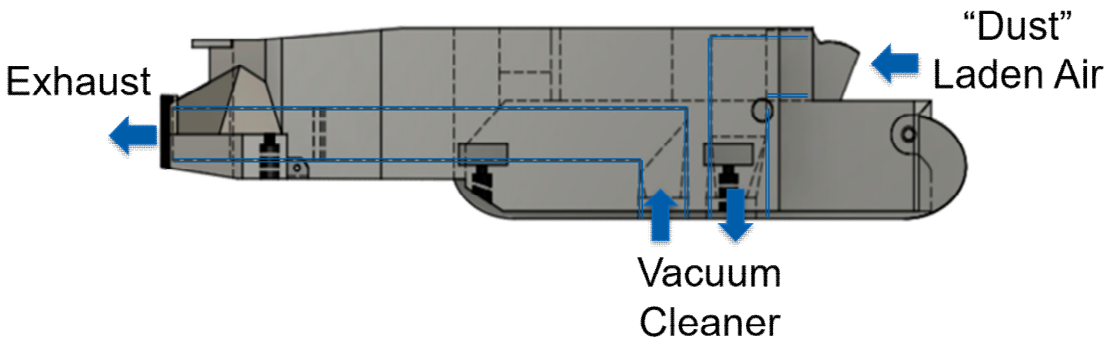

Figure 3.8 Schematic of scrubber design

3.6 Particle Image Velocimetry Principles

PIV is an optical method of flow measurement and visualization. It offers a non-intrusive method for obtaining velocity fields by measuring the velocity of particles seeded into the airstream. These particles are illuminated by a sheet laser, and an image is captured of their current position. Laser pulses and image captures are synchronized and produced in pairs called frames. The time delay between captures, or ΔT, is known, and therefore, the displacement of the particles between capture produces a velocity vector.

The selection of ΔT is very important for proper capture. At lower airspeeds, a relatively large ΔT must be used because the particles take a relatively longer time to move the required number of pixels for accurate analysis. Likewise, when the air velocity is high, the ΔT must be smaller. Multiple air speeds (i.e. a jet stream) requires more images to cancel out errors; or the analysis should include more than one ΔT.

3.6.1 Image Processing

Images are calibrated to correlate the image size (in pixels) to real world dimensions. Calibration is required any time the laser sheet height is changed. This is done by placing an item of known size at the same height as the laser.

Images are pre-processed to extract and remove background information from the images. The background is anything that remains constant between image pairs, such as reflections and stationary objects, e.g. the continuous miner (Honkanen & Nobach, 2005). A background image is generated by extracting the minimum or average intensity of the gray scale images. The generated background image is then subtracted from the image and all subsequent images, isolating pixels with the highest intensity. The progression is shown in Figure 3.9 whereby the raw image is on the left, the generated image in the middle, and the pre-processed image to the right.

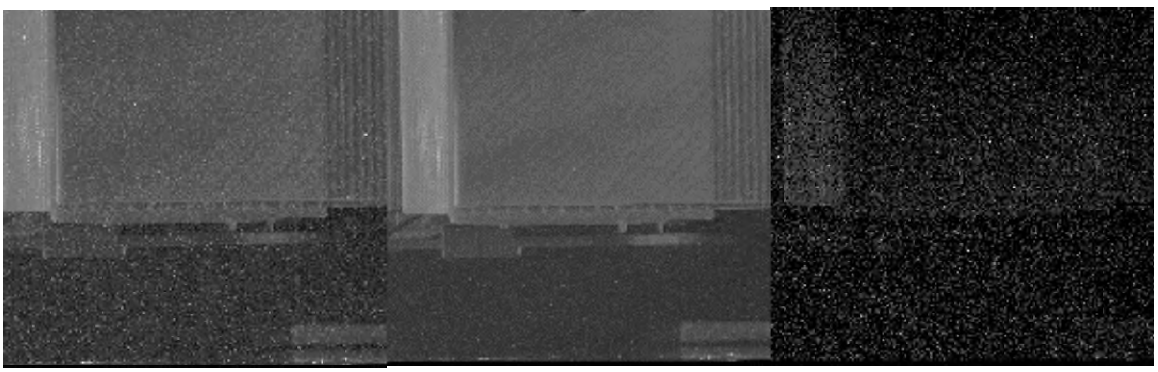

Figure 3.9 Progression of image pre-processing by background subtraction

Pre-processed images are passed to the image processor where each image frame is processed using the setup shown in Figure 3.10.

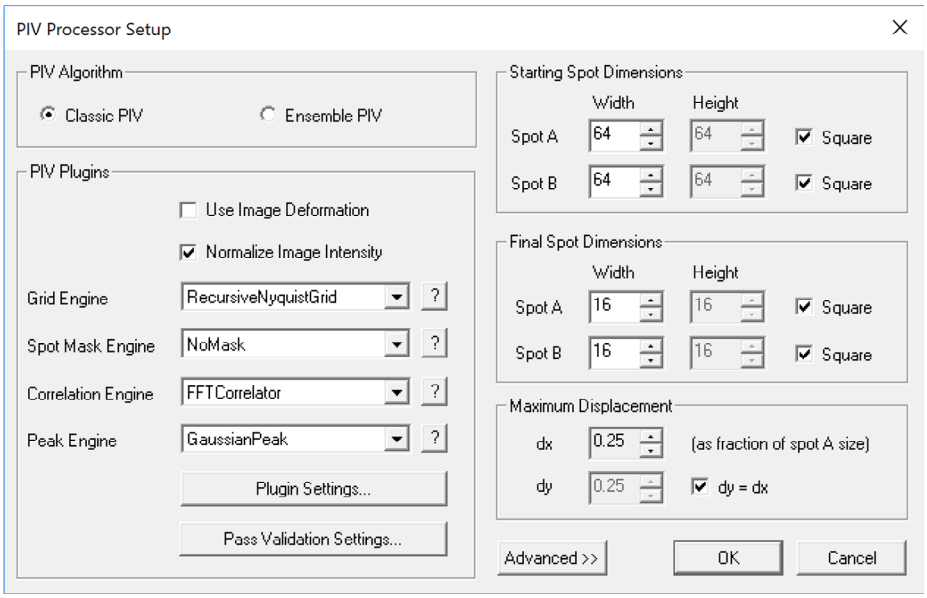

Figure 3.10 PIV Processor Setup

In all analyses presented in this dissertation, the image correlation analysis was performed with a standard Fast Fourier Transform (FFT) algorithm. Using a Recursive Nyquist Grid Engine, images are divided into investigation windows as a 64x64 pixel grid, as shown in Figure 3.11. These areas are processed again using a 16x16 pixel grid. The grid engine processes the images in two or more passes that begins with a 50% overlap. The results of the first pass are used to optimize the spot offsets of subsequent passes.

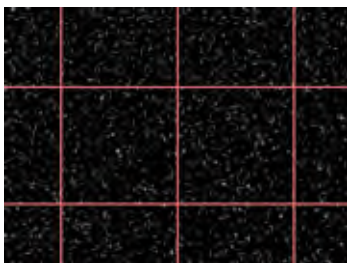

Figure 3.11 Image is segmented into investigation windows by 64x64 pixel grid.

Spots from the correlation engine are passed to the peak engine to measure the displacement. Peak engines determine the peak location in the correlation map as shown

in Figure 3.12. GaussianPeak is the recommended peak engine for use with the FFT Correlation Engine (TSI Inc., 2014). The Gaussian peak equation is given by Equation 3.9.

$$dx = x + \frac{\log l - \log r}{2(\log l + \log r - 2\log c)} - x_0 \tag{3.9}$$

where l, r, and c are intensity values for the left, right, and peak pixels in the correlation map, x is the integer shift, and x_0 is the zero-shift location. The threshold set for the maximum peak to noise ratio was 1.5. The resulting vectors are validated using the median test and a neighborhood size of 5x5. This measures the difference between the vector and surrounding vectors. If the result is out of tolerance, then it has failed validation.

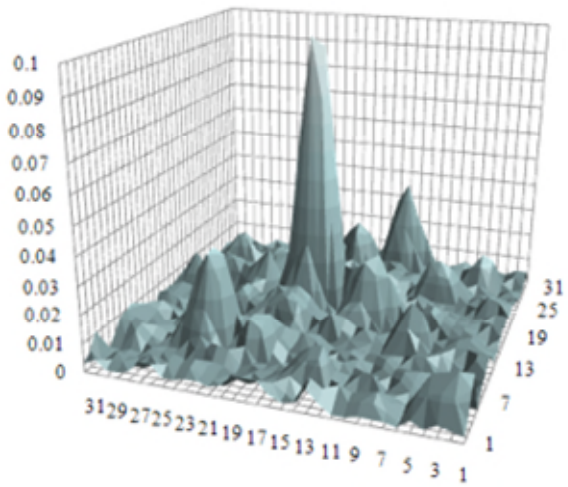

Figure 3.12 Correlation Map (Troolin, Hortensius, & Lai, 2020)

Vector conditioning was used to fill holes and smooth the vector field. These are represented as yellow-colored vectors in Figure 3.13. Green ones are passing vectors. The vector field is saved for each image pair as a .VEC or .BVEC, if the binary format was the selected, file type.

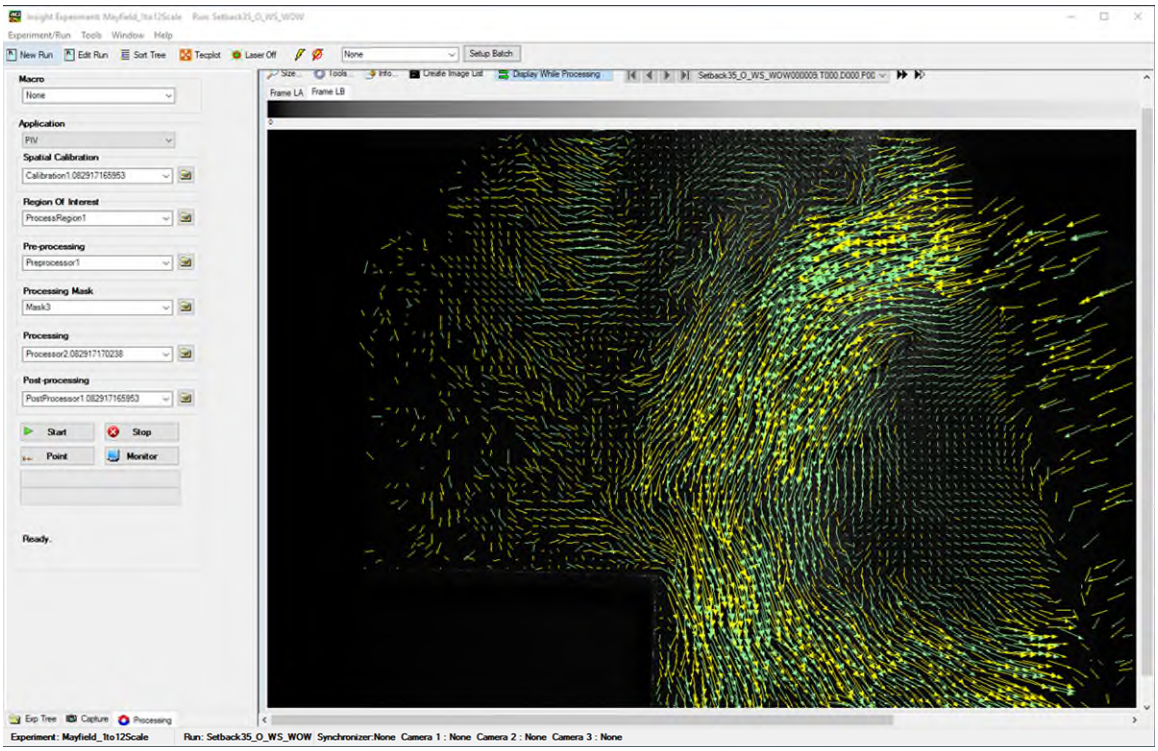

Figure 3.13 Velocity vector field output.

3.6.2 Tecplot

Tecplot is used for visualizing the vector field. Using the TSI PIV plug-in, Tecplot can accept the exported vector field (.VEC files). The plug-in loads the files and allows the user to perform calculations on them. To perform the steady state analysis, the plug-in is used to create an average vector field of all valid data.

The resulting layouts can be exported as images and are the source of most PIV images in this dissertation.

3.7 Instrumentation

3.7.1 Particle Generator

The seed particle generator, sometimes called a bubble generator, produces the florescent aerosolized particles needed to perform the PIV experiments. The generator used in this experimental setup is a TSI model 9307-6, shown in Figure 3.14. This unit can produce large volumes of aerosolized olive oil or salt particles using a laskin nozzle. The reservoir is filled with olive oil and pressured air produces droplets which are sized using an impactor before leaving the unit. This provides a consistent particle size regardless of user-controlled pressure. An increase in pressure produces more particles while lower pressure reduces the concentration. The desired release rate, and thus concentration, is a factor of the air velocity, and must be calibrated at each new air speed.

Figure 3.14 Seed particle generator.

3.7.2 Synchronizer

The synchronizer, a TSI LaserPulse Model 610036, coordinates and triggers the laser and camera within the timing parameters set within the TSI Insight 4G ® software.

3.7.3 Laser

The Nd:Yag (neodymium-doped yttrium aluminum garnet) laser provides the light necessary to illuminate the particles. Initial experiments were conducted using a NewWave Research Solo III 15 Hz Laser which was replaced by a NewWave Research Gemini 15 Hz Laser. The first laser is no longer serviceable and broke during early testing. There is no significant difference in these two lasers in this application. These lasers produce a 532 nm wavelength (green) interval light.

Figure 3.15 (left) Laser controls and (right) laser head.

Modular 610026 light sheet optics consisting of a collimator and two cylindrical lenses (-15mm and -25mm) are used in tandem to develop a thin laser sheet of uniform thickness. Figure 3.16 shows their installation configuration as determined by the vendor for this application's dimensions and camera.

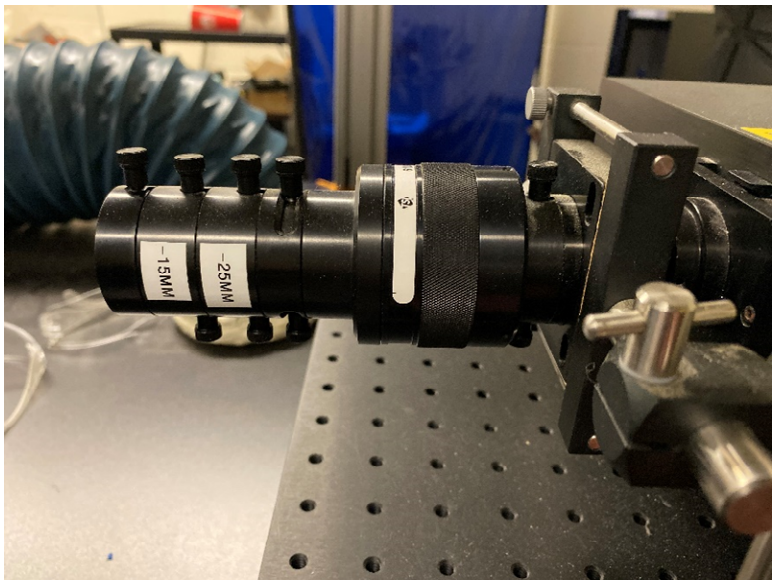

Figure 3.16 Laser lens and collimator.

3.7.4 Camera

A PowerviewPlus 29MP-HS camera is used for capturing PIV images. Figure 3.17 shows the camera's installation above the model. The track system allows the camera to move to capture various areas of the model. The area of the scale model is too large to capture in one image without camera induced distortion within the study area.

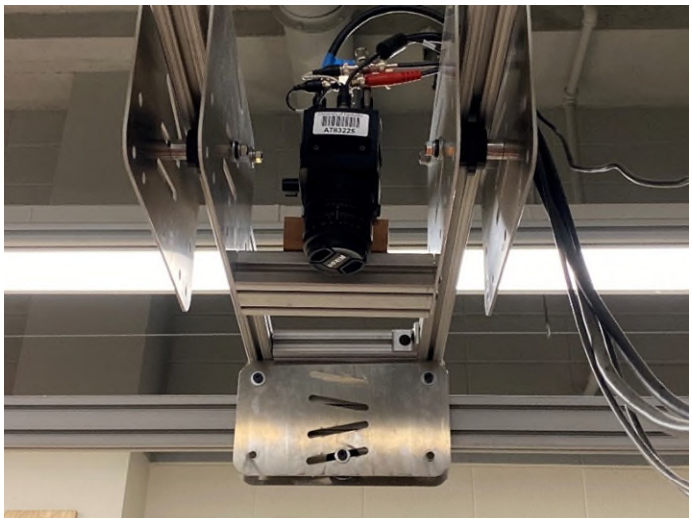

Figure 3.17 CCD camera installed on track above model.

3.7.5 Frame Grabber

The Xcelera-CL + PX8 is the frame grabber used with the PIV camera. It is installed directly into the computer mother board of the PIV control computer. Frame grabbers are necessary for these applications due to the speed at which data needs to be transferred and to facilitate the frame straddling (TSI, 2013). They are responsible for directing the images directly to memory freeing up the computer CPU for completing other tasks. This is especially important when capturing and transmitting high resolution images in real time such as in the PIV application.

3.7.6 Velocimeters

Air velocity readings were taken using a hot wire anemometer. This type of anemometer is very accurate (±3% of the reading) for both low and high velocities. TSI model 9565-X and model 9545 were utilized in this experiment. The 9565-X has data logging capabilities and can also calculate turbulent intensity.

Figure 3.18 TSI velocimeter with telescoping wand.

3.8 Procedure for PIV Image Collection

The laser head(s) are turned On to start the cooling pumps and warmed up the internal gasses. Per the manufacturer's instructions, the laser warm up must complete before starting the PIV experiment. The curtain setback and offset, the continuous miner and the slab wall are arranged for the specific experiment.

The polycarbonate top is gently placed on top of the model over the entry portion of the model. The polycarbonate has holes placed along the edge approximately 1.5 to 2 inches from the rib wall. The TSI hot-wire anemometer probe is inserted through the hole for measuring air velocity. The fan for the model is turned on, and air is circulated through the model for a minimum of 30 seconds to reach steady state conditions. The fan speed is adjustable via a single-phase fan controller and a potentiometer.

The fan speed is adjusted until the line brattice air velocity is steady, and fluctuations stay within approximately ± 5 ft/min of the target velocity. A turbulence intensity enhancer is installed in the intake cross-cut to intentionally increase turbulence.

Its purpose is described in Section 4.2. The polycarbonate sheet is replaced with a glass top. The glass has greater clarity and cleanability, which is required for the PIV images. Air velocity between the line brattice and the rib is measured while the polycarbonate sheet is installed because there is no other method established to measure it once the top is replaced with a solid glass pane, without the measurement ports.

The laser power is set to zero and initialized to begin the computer control of the firing of the laser beam pulses. When computer control is established, the laser is set to full power. Safety glasses which are designed for the laser light spectrum are required past this point. The lens cap and shutter cover are removed. They are left on up to this point to protect the camera and operator from stray beams. The air hose from the laboratory's compressed air supply is attached to the atomizer and pressurized. (Previous experimentation was performed to adjust the release rate for fresh air intake volume, which is controlled by a regulator.)

To begin the PIV testing, the room is first secured to prevent entry of unprotected people. Tests are performed in complete darkness so that the particles are only illuminated by the laser. TSI Insight 4G is used to control the equipment. The test is configured. A series of initial runs are performed to determine the ΔT which permits a selection of particles to be easily tracked between frames. Using that ΔT, 250 image pairs are captured for the test condition. The camera field-of-view is not sufficient to capture the entire testing area in one picture without distortion so two precise camera locations are used, one capturing the head of the miner called the "inby" region (Figure 3.19b) and the other at the tail of the miner in the "outby" region (Figure 3.19a).

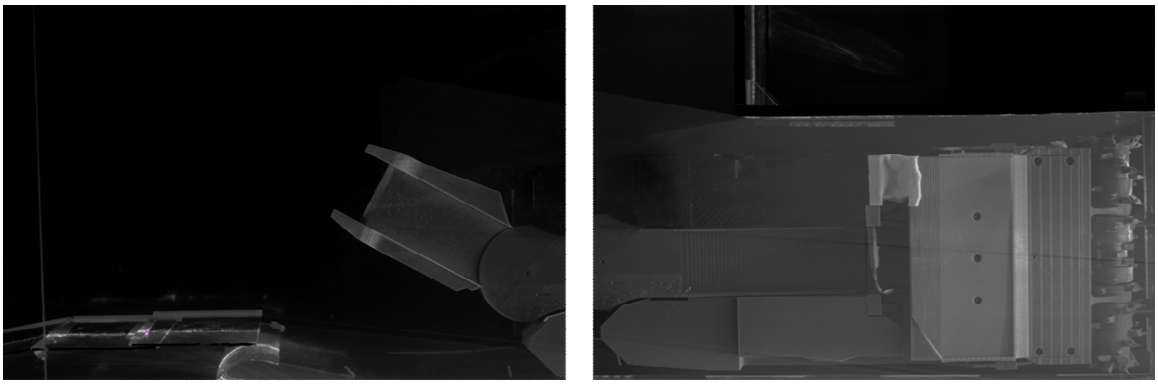

a b

Figure 3.19 Processed background images showing the camera capture regions in the outby (a) and inby (b) areas.

Determination of ΔT is repeated for each camera position. When the mine face is moved, changing the distance from the line brattice, the procedure of determining ΔT and capturing the images from two locations is repeated. The mine face is moved by sliding the faux floor out in set increments.

After the images are collected, during post-processing, they are analyzed by the software and the vector fields are generated by the means described in Subsection 3.6.1.

The background images for each test were imported and merged to establish the displacement of the outby images as the PIV processing does not account for this. The displacement of the background was used to also merge the processed velocity zones. Streamlines were created to visualize the airflow through the model and made to overlay the background images for reference.

3.9 Test Conditions Examined

The purpose of the study was to study the airflow patterns under two main influences: with an active device, the dust scrubber; and with a passive device, the wing

regulator, over the course of a complete cutting cycle. This type of study would be very difficult in the field and at full-scale and would not offer the vector field resolution of PIV testing.

Based on field surveys, all tests target an air quantity behind the curtain of 10,000 CFM. As shown in Table 3.1, this airflow quantity remains turbulent (Re is greater than 4,000) even under Froude scaling. Three scrubber ratios were chosen for testing: 85%, 100%, and 115% of the curtain air quantity. These simulate underpowered and overpowered conditions, which cause poor performance and recirculation.

The wing regulator passively accelerates air towards the face. A series of experiments were performed to simulate its influence on its own and then its combined interaction with the scrubber. A scale model of the wing regulator was created by scaling a design drawing from the inventors and 3D printing the ventilation control used in the scale-model experiments. The setback was divided into four distances: 27-ft, 32-ft, 37-ft, and 40-ft. Each subsequent power testing, scrubber active, was performed at each setback except at 27-ft with the wing, which could not be accommodated.

CHAPTER 4. RESULTS

This chapter contains data and analyses from the experimental procedures described in the previous chapter. Not all data collected is included for space, raw data will be placed in archival storage for potential future analysis.

4.1 Field Study Results

The diagrams in Figure 4.2 and Figure 4.1 illustrate the flow patterns and velocity field captured at the empty entries of Mines 2 and 3, respectively. Just like in Mine 1, flags were attached evenly distributed to roof bolts in the entry to visualize the airflow. Air quantity behind the curtain (five feet from the setback) was measured at the beginning of each test three times and averaged. The entry height and width were measured. A TSI 9535 velocity meter was used to measure the airflow along the ribs taken at approximately two feet from each rib at five-foot spacing from the curtain to the face (or as close to the face as could safety be taken). Positive velocity values denote air flowing in the inby (towards the face) direction and negative velocity values denote air flowing in the outby (towards the curtain) direction.

Despite the large difference in curtain quantity and differences in dimensions, the air follows a similar path. This pattern was also seen at Mine 1 (Figure 3.1). As the fresh air exits the line brattice, it quickly separates from the rib turning to the left and splits along the left rib. This creates a zone of slow-moving, recirculating air by the face.

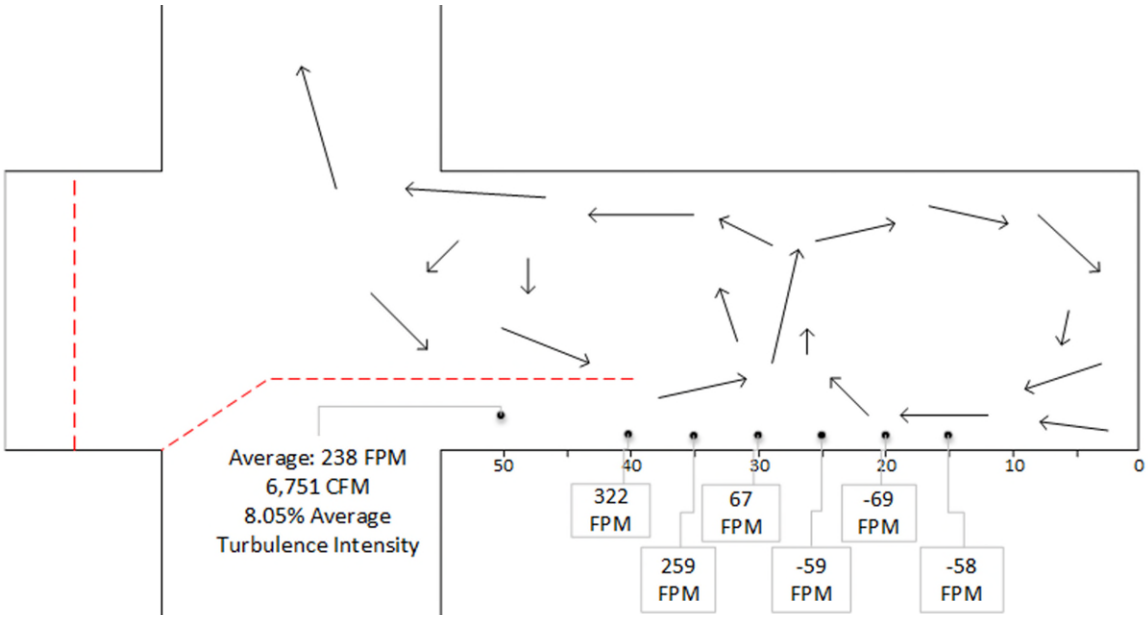

Figure 4.1 Diagram of testing results for Mine 2 without wing regulator or CM.

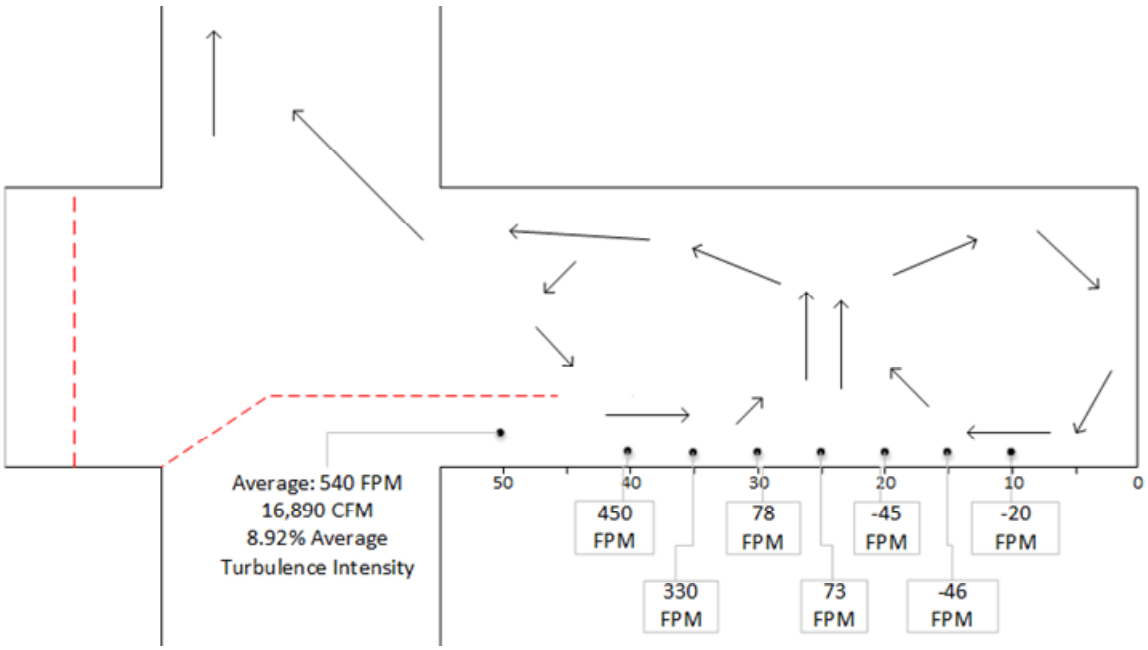

Figure 4.2 Diagram of testing results for Mine 3 without wing regulator or continuous miner.

Velocity data was extracted from the curtain-side rib for the empty entry scenarios. To account for curtain quantity differences, the velocity was normalized as a percentage of the average curtain air velocity measured at each mine, e.g., 238 fpm for Mine 2 and 540 fpm for Mine 3. Air

flowing inby is considered positive and air flowing outby is negative. The sample points were also normalized as a percentage of the total setback, with 0% representing the face and 100% representing the opening of the line brattice. This methodology allows the field data to be analyzed together, establishing a relationship between the distance the air travels and the rate at which the curtain air (e.g., fresh air) velocity drops. Figure 4.3 shows this relationship.

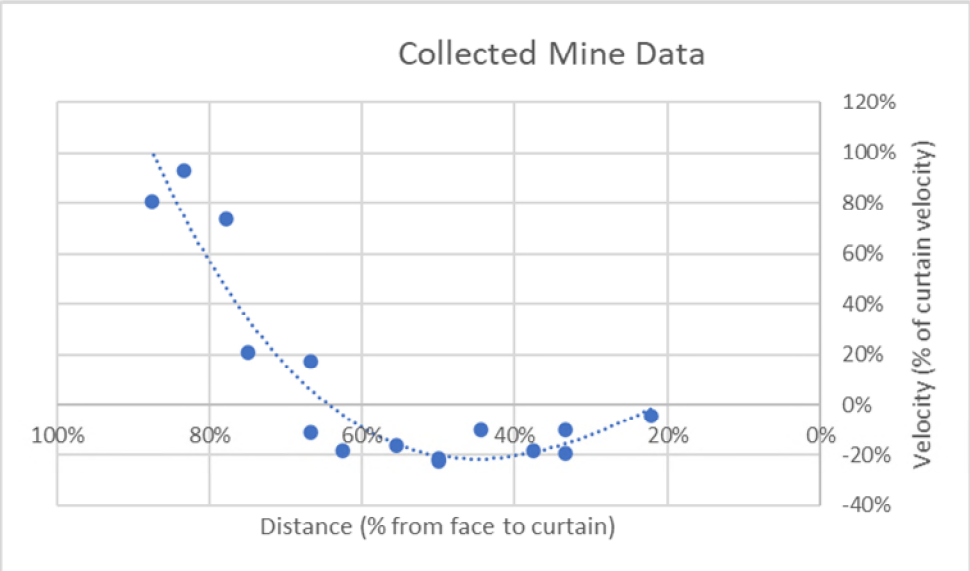

Figure 4.3 Tight side velocity curve of field studies without wing regulator or continuous miner.

When compared in this way, it is evident that the air velocity follows a very similar pattern despite the differences in geometry and curtain air quantity. Inspection of this figure shows that the inby air velocity drops to zero at approximately 70% from the face. This loss of inby velocity causes the air to flow toward the exhaust, meaning that the air is not sweeping the face as intended. This is referred to as the point of separation in this dissertation.

4.2 Turbulent Intensity Control

It was observed that the airflow patterns in both the Dust Gallery, which is the full-scale model, and the reduced scale model did not match those observed at the three mine sites presented

in Section 4.1. The field tests also measured turbulence intensity (TI) in the tight side of the line brattice. Turbulence intensity in the Dust Gallery was measured at 3-5%, but in the mines, this value was at 8-12%.

Experiments to increase the TI were conducted on the lab scale model. A system of a baffles, called a turbulence intensifier, was installed in two configurations, as shown in Figure 4.4, to effectively add additional length to the intake without extending footprint of the model. The testing was considering two variables: wall roughness and shock loss. The 1/12th scale model is made of acrylic and inherently smooth. Sandpaper sheets were attached to the rib walls to increase roughness.

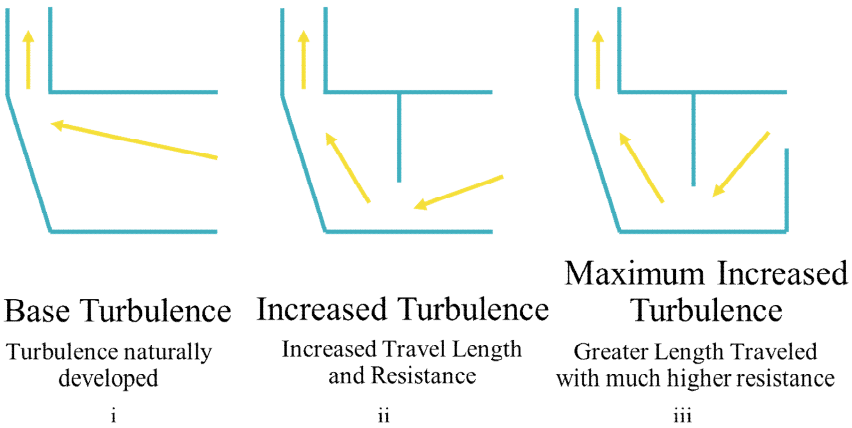

Figure 4.4 Configuration of baffles to increase turbulence.

For each condition, shown in Figure 4.4, turbulence intensity was measured on the tight side of the line brattice. The results are shown in Table 4.1. While the addition of the 60-grit sandpaper (rough) increased the TI as expected, the number of baffles made a greater impact on the TI. In addition, the sandpaper had a very small impact at the configuration of iii (two baffles at the intake), indicating that the sandpaper would not be necessary in this

configuration. This is significant because the sandpaper caused issues with the PIV measurements by reflecting the laser light.

Table 4.1 Turbulent Intensity Results

Test	A	B	C	D	E	F
Wall	Smooth	Smooth	Smooth	Rough	Rough	Rough
Baffle Configuration	i	ii	iii	iii	ii	i
Measured TI	1.33%	1.55%	3.34%	3.43%	1.94%	1.65%

Velocity measurements in the $1/12^{th}$ scale model along the line brattice-side rib were extracted from the PIV data and plotted in Figure 4.5. Inspection of this figure shows similarity in the velocity curve among the tests and the field survey. Test B, which used the smooth-wall and one baffle, had the closest point of separation. The turbulence intensity enhancer was installed for the remainder of the PIV tests discussed in this chapter. It is noted that this is not the condition having the highest turbulence intensity; however, it is the one having the closest separation point compared with field data.

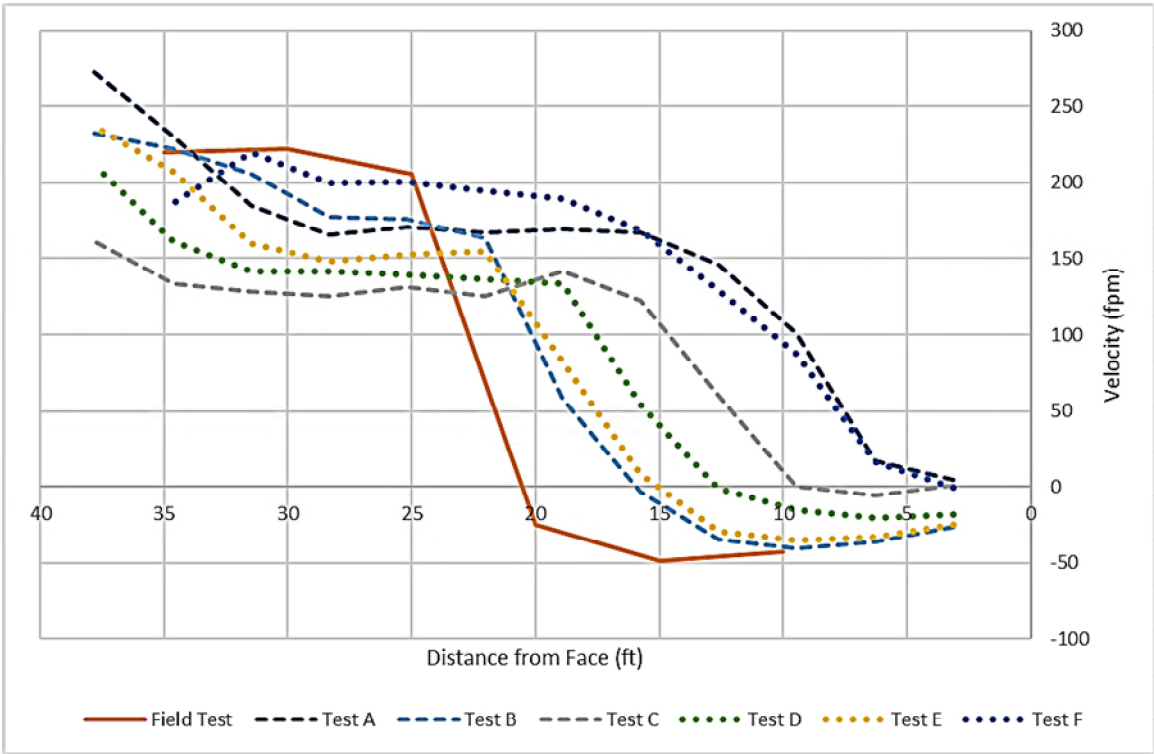

Figure 4.5 Velocity measured at points across the model and in the field.

In the full-scale model, a similar turbulence intensifier was constructed which resulted in the full-scale model accurately matching the field tests. In the full-scale testing, corrugated roofing material was added to the walls for roughness, which did not interfere with the model's operation and is still installed. The turbulence intensifier and the roughness alone were not able to replicate the observed air patterns in the full-scale model. Whereas, in the 1/12th model, the turbulence intensifier alone was sufficient.

4.3 Full-Scale Test Results

As with the mine-site field studies, all full-scale tests were conducted at the deepest point of the cut, i.e., a 40-foot setback. Tests that included the scrubber were operated at an approximately 85% ratio of scrubber-air to curtain-air quantity.

4.3.1 Box Cut without Wing Regulator, Scrubber Off

Figure 4.6 shows a representative example of the full-scale tests for a box cut with the scrubber inactive and without the wing regulator. For this test, the average curtain air velocity was 291 fpm (or 8160 cfm). As shown in this figure, the fresh air separates from the rib near the right rear corner of the continuous miner, flows toward the slab and splits, with the majority of the air flowing to the return. This leaves an area with little to no flow except for recirculation.

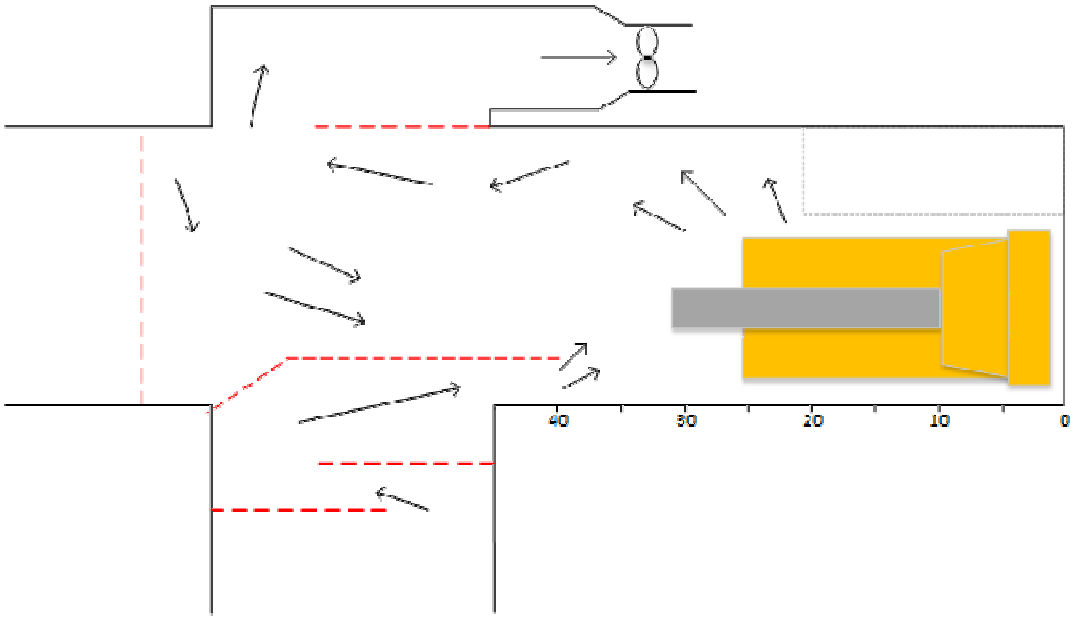

Figure 4.6 Dust Gallery test, scrubber inactive, without wing at 8,160 CFM curtain air quantity.

4.3.2 Box Cut without Wing Regulator, Scrubber On

Figure 4.7 shows a representative example for the box cut with the scrubber On and without the wing regulator. For this test, the average curtain air velocity was 303 fpm (or 8475 cfm), and the scrubber air quantity was approximately 7000 cfm. With the scrubber activated, the separation point is significantly closer to the face than in the previous test (Section 4.3.1), occurring approximately 10 to 15 feet further into the box cut. Unfortunately, airflow within 15-ft of the face was too turbulent to determine the flow direction. Eddy formation in the outby area adjacent to the curtain was also observed.

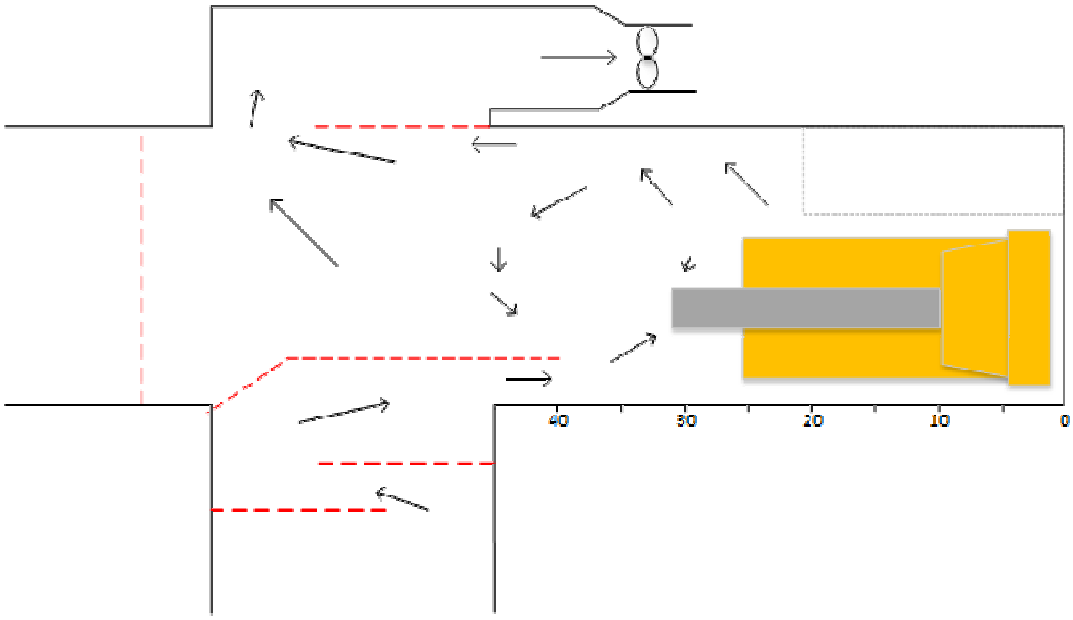

Figure 4.7 Dust Gallery test, scrubber at 7000 CFM, without wing and 8,475CFM curtain air quantity.

4.3.3 Box Cut with Wing Regulator, Scrubber Off

Figure 4.8 shows a representative example for the box cut with the scrubber off and with the wing regulator. For this test, the curtain air quantity was 7180 cfm, and the curtain air velocity was 256 fpm. When the wing regulator was implemented, without the scrubber, the fresh airflow penetrated further into the box cut; however, it still separated in approximately the same area as the previous test, or about 15 to 20 feet from the face (Section 4.3.2).

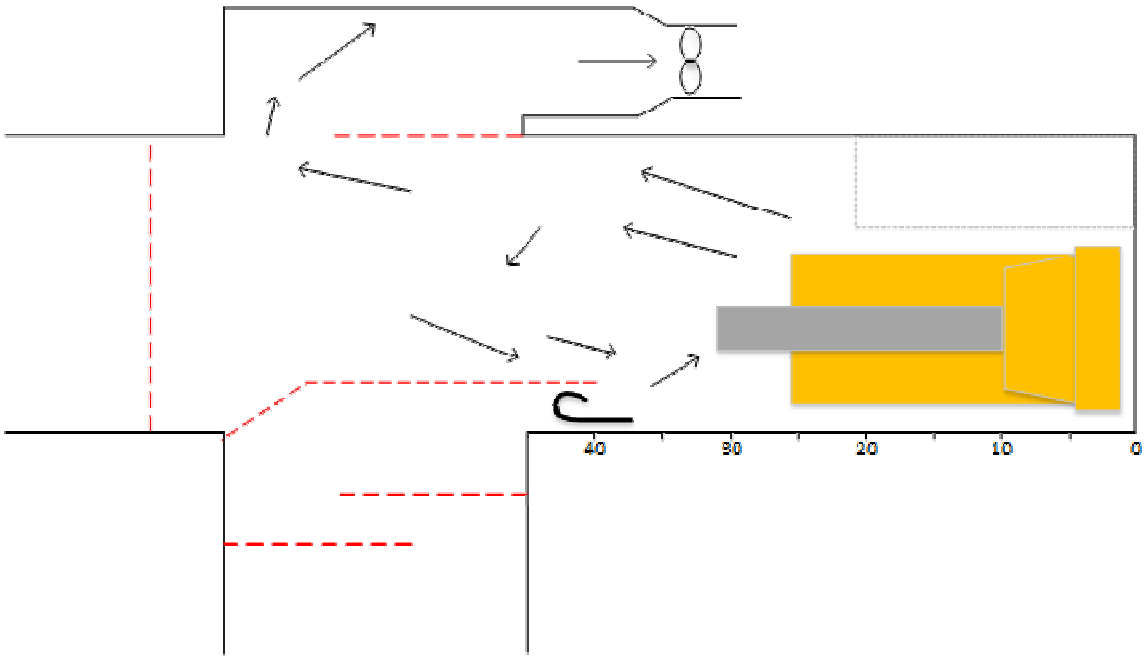

Figure 4.8 Dust Gallery test, scrubber inactive, with wing regulator at 7180 CFM curtain air quantity.

4.3.4 Box Cut with Wing Regulator, Scrubber On

Figure 4.9 shows a representative example for the box cut with the scrubber on and with the wing regulator. For this test, the average curtain air velocity was 263 fpm (or 7364 cfm), and the scrubber airflow quantity was approximately 7,000 cfm. With the wing regulator and scrubber both activated, the air travelled inby the curtain side rib and is noted to have traveled outby the slab side. Turbulence inby the 15-ft mark prevented directional readings.

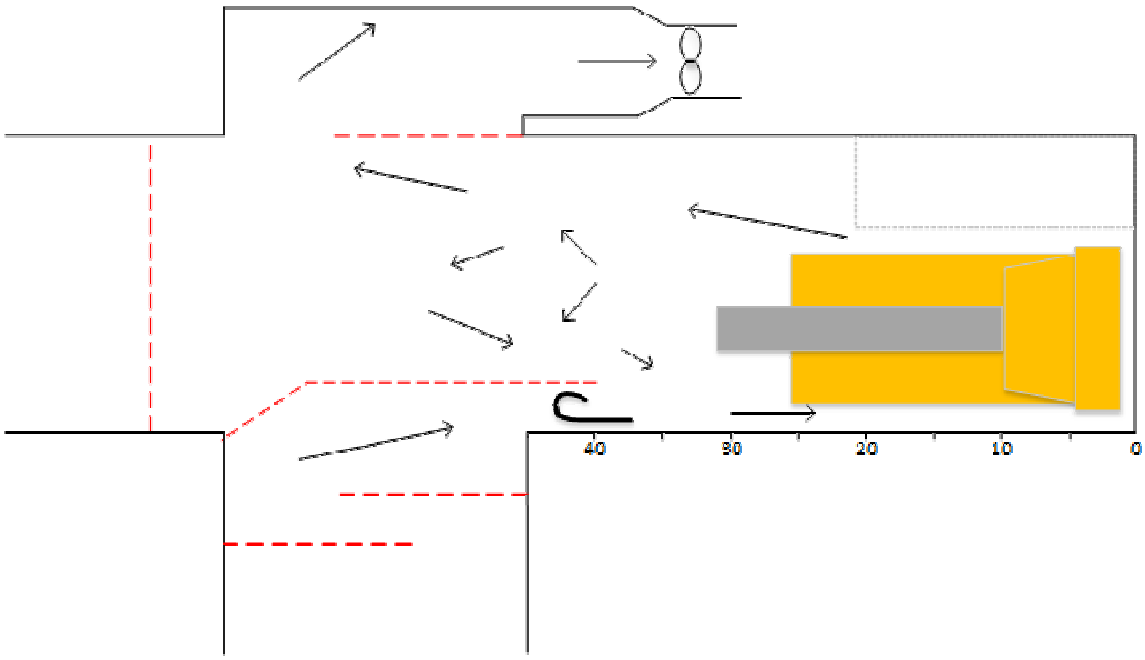

Figure 4.9 Dust Gallery test, scrubber at 7,000 CFM, with wing regulator and 7364 CFM curtain air quantity.

4.4 Reduced-Scale Model: Unaided Face Ventilation

Figure 4.10 presents the results with the air scrubber off and without the wing regulator. These images were generated from vector data collected and processed from PIV data which were averaged to develop the streamlines. The number of image pairs used by the software to calculate the averaged vectors is in the corner, only vectors containing at least 80% of the valid of samples were used. This means that if there were 100 image pairs taken and a sector had 79 (or less) measured vectors returned from processing, it was masked from the result.

Inspection of Figure 4.10 illustrated how the airflow patterns change as the continuous miner extends the box-cut. In each case, the majority of the fresh air penetrates flows to a point slightly inby the beginning of the box cut before separating and flowing towards the slab. With

the 27-ft setback, the air flows to the face area and recirculates in a clockwise rotation near the CM cutting drum. As the cut depth is increased, this area of recirculation widens as high velocity air is directed out to the return. This is the resulting pattern also in the 37-ft and 40-ft setback. Note that at the 37-ft and 40-ft setback distance, the reduced velocity of this recirculating air made it difficult to keep enough particles suspended and concentrated to accurately measure the flow in this region. Additionally, particles in this region do not stay in the same z-plane. This results in a loss of data to the PIV system. Although this is problematic for PIV testing, it does support the notion that, at high setback distances, the area near the face has a significant amount of slow-moving, recirculating air that could cause an accumulation of methane.

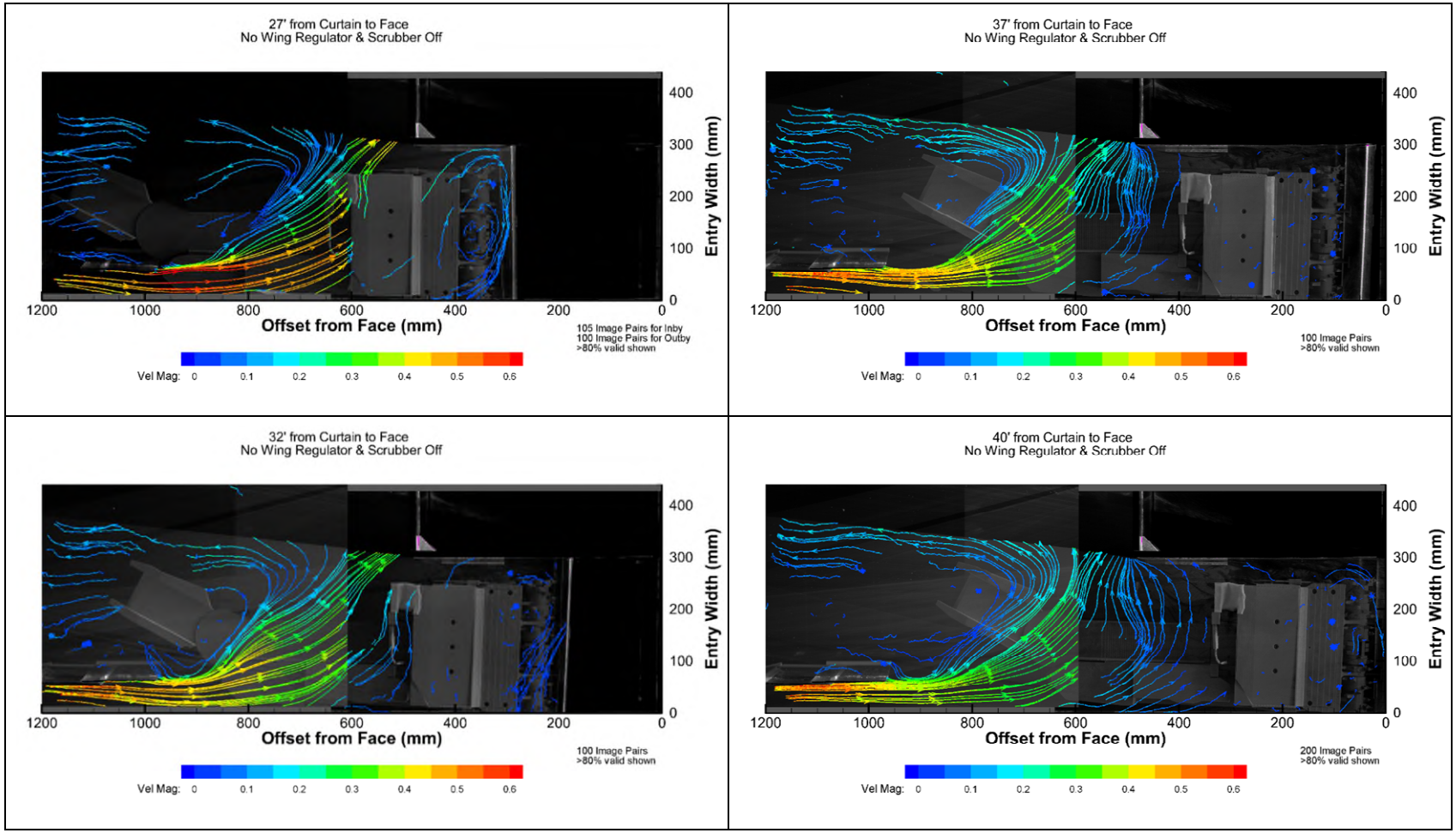

Figure 4.10. Streamline exports from Tecplot ® that illustrate the airflow changes during the progression of the box cut without the wing or scrubber installed.

4.5 Reduced-scale Model: Scrubber impact on face airflow patterns

In this series of tests, the air pattern was measured for full-scale equivalent setback distances of 27-ft, 32-ft, 37-ft, and 40-ft with the scrubber fan setting intended to simulate a condition of 85%, 100%, and 115% scrubber to curtain air ratio. During the experiment, 200 image pairs per setup were averaged to illustrate the most likely airflow pattern. As previously done, only sectors, which contained vector results with more than 80% (or at least160 valid measurements), were kept in the final results shown in the following subsections.

4.5.1 85% Scrubber Ratio

In this scenario, the cut progresses with the scrubber set to 85% of the target air volume at the curtain. The results of the average PIV produced vectors are shown in the streamline diagrams in Figure 4.11. Immediately in the 27-ft setback image, an eddy has already formed on the curtain side. This may be an example of the curtain air overshooting the scrubber. As the miner's cut deepens, curtain air separates from the curtain side rib and flows to the left. Majority of the fresh air is drawn immediately to the left-hand scrubber vent. The eddy of slower moving air becomes larger as the cut is extended.

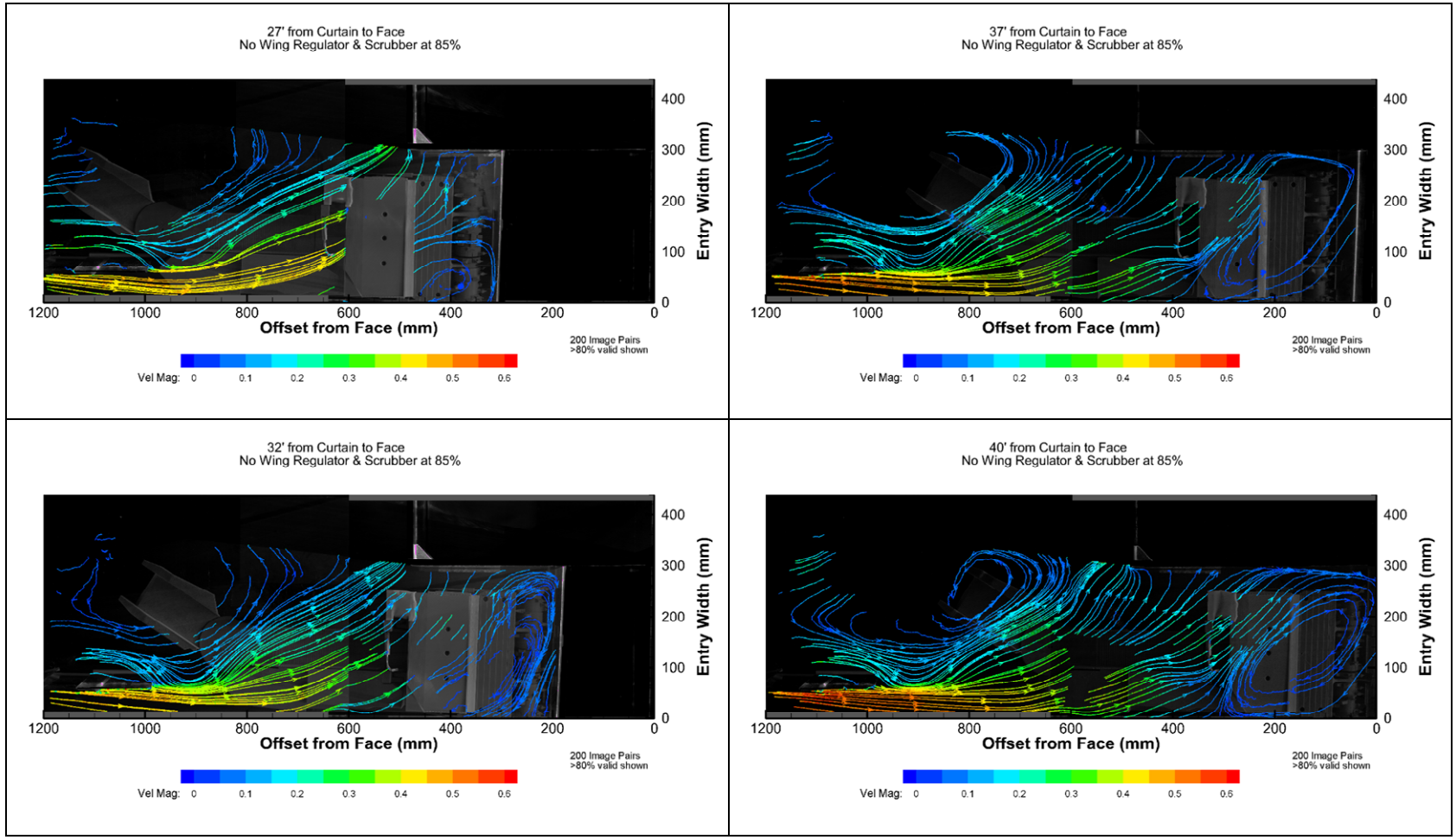

Figure 4.11 Streamline exports from Tecplot ® that illustrate the airflow changes during the progression of the box cut without the wing with the scrubber nominally set at approximately 85% of the target curtain velocity.

4.5.2 100% Scrubber Ratio

The air pattern was measured for 27-ft, 32-ft, 37-ft, and 40-ft setback with the scrubber fan setting intended to simulate a condition of a one-to-one ratio of scrubber air to curtain air volume. Figure 4.12 shows the progressive changes to the airflow over the tested setbacks. At the beginning of the cut, the PIV image shows that the fresh air is pulled to the face where it sweeps the face to the left before accelerating towards the vent area of the continuous miner scrubber.

As the cut progresses, the zone of fresh air widens, and an eddy forms in the curtain side corner of the face. It is also notable that the air velocity seems to be greater in the images with the greater setback. This will be further evaluated in the next section. While relatively high velocity air continued to supply fresh air to the face, the eddy continued to grow. Eddy development in face areas are zones of recirculation which can trap and accumulate contaminates.

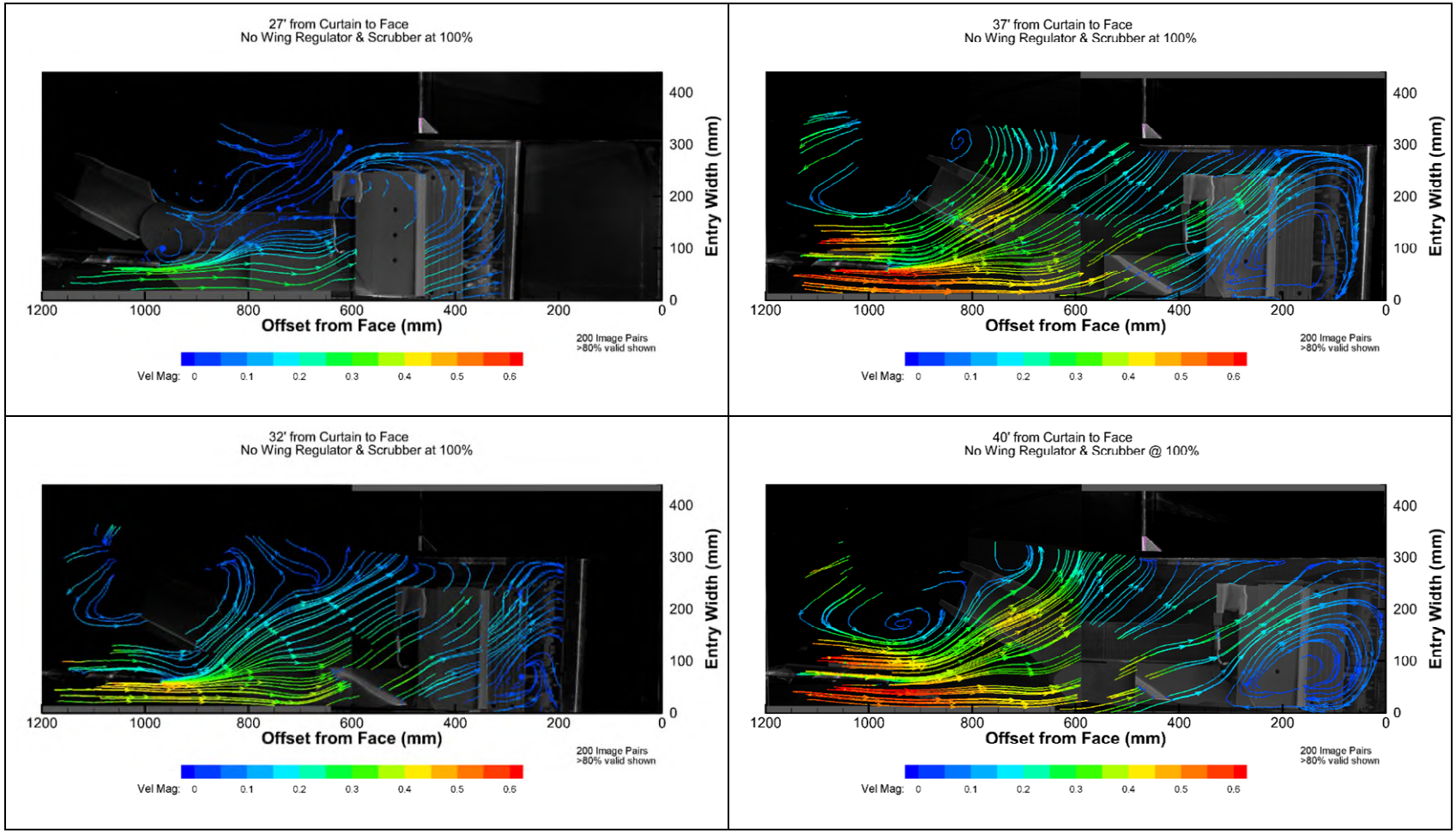

Figure 4.12 Streamline exports from Tecplot ® that illustrate the airflow changes during the progression of the box cut without the wing with the scrubber nominally set at approximately 100% of the target curtain velocity

4.5.3 Scrubber at 115%

The results of the average PIV produced vectors are shown in the streamline diagrams in Figure 4.13. For the scrubber intake at approximately 115% of the curtain air volume, as with the 100% ratio test, the fresh air reaches the face area before flowing into the left scrubber inlet; however, the curtain air is joined by high velocity air from the off-curtain side. This is due to the additional pull from the scrubber. There is also eddy formation present in the curtain (right) side of the face near the right scrubber vent. In these streamline diagrams, the vortex formed by the scrubber exhaust is present. It is also experienced in the full-scale model and real mines.

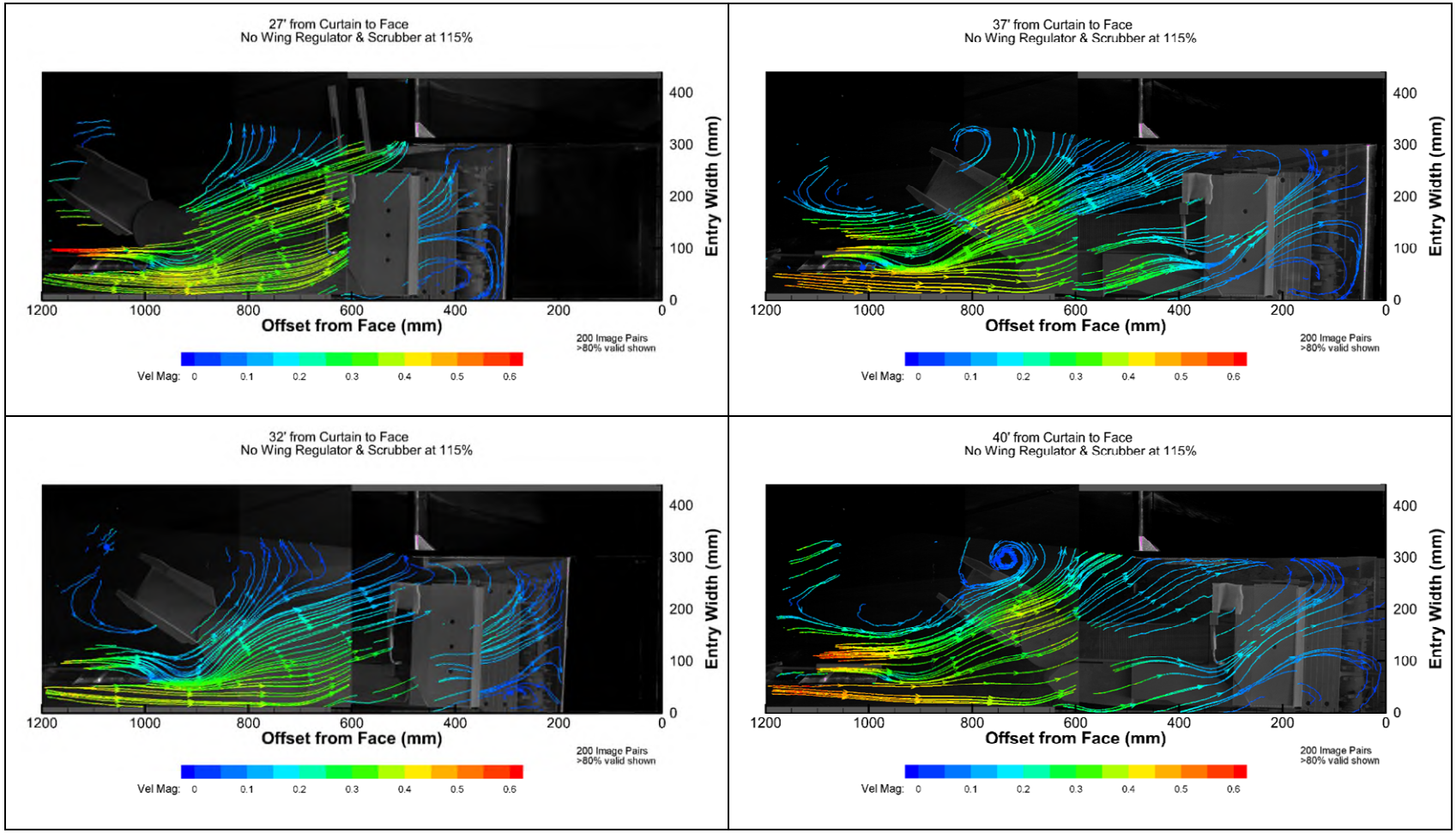

Figure 4.13 Streamline exports from Tecplot ® that illustrate the airflow changes during the progression of the box cut without the wing with the scrubber nominally set at approximately 115% of the target curtain velocity.

4.6 Scaled Model: Passive Wing Regulator

The next experiment models a continuous miner face which utilizes a blowing face with only the wing regulator while the scrubber is off. The PIV results are shown in Figure 4.14. With the wing regulator in place, fresh air is accelerated towards the face. At the 32-ft setback and below, the curtain air flows to the face, sweeping across the face before flowing to the return. However, as the box cut becomes deeper, the fresh air does not reach the face, and a large eddy is formed in front of the CM.

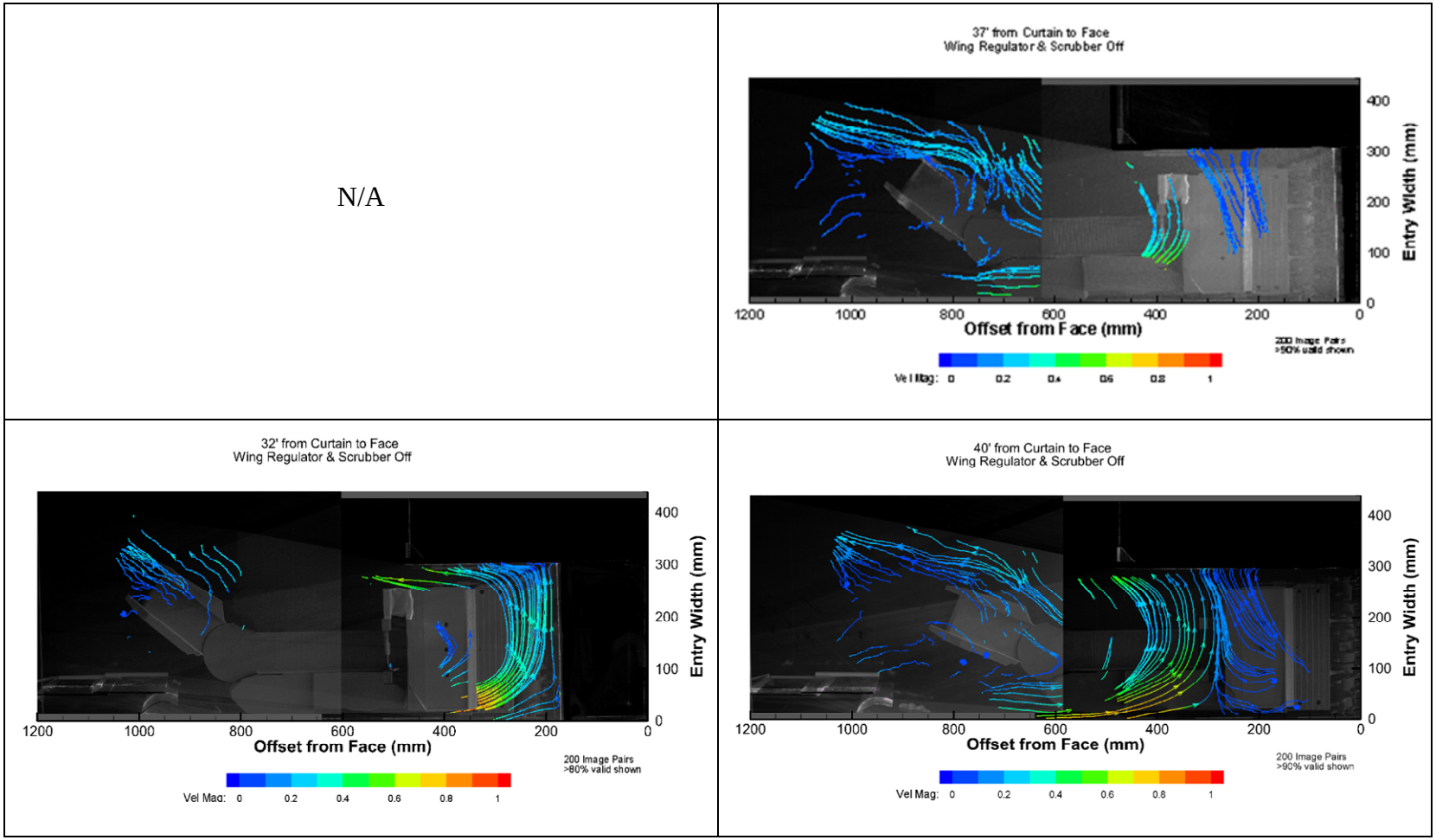

Figure 4.14 Streamline exports from Tecplot ® that illustrate the airflow changes during the progression of the box cut with the wing with the scrubber off.

4.7 Scaled Model: Combined Wing Regulator and Scrubber Effect on Face Ventilation

The next series of tests were designed to test the effects of combining both a passive regulator and the scrubber at power levels 85%, 100% and 115% of the target curtain-air volume. In these tests, only the 32-ft, 37-ft, and 40-ft setbacks were tested. As in the previous test, a 27-ft setback was not tested, as the placement of the wing regulator does not allow the continuous miner to be positioned at this location.

4.7.1 85% Scrubber Ratio

Figure 4.15 shows the average velocity calculated for three setbacks: 32, 37, and 40 feet at a scrubber to curtain ratio of 85%. Immediately it is noticeable that the PIV system was not able to properly capture particle travel in the horizontal plane. In this setting, the air is progressing toward the face and sweeping it until the full depth is achieved. The effect of the wing, combined with the vacuum of the scrubber, assist the air to flow further into the box cut. However, the PIV is not able to process the face area due to the high turbulence as also observed in Dust Gallery and described in Section 4.3.4.

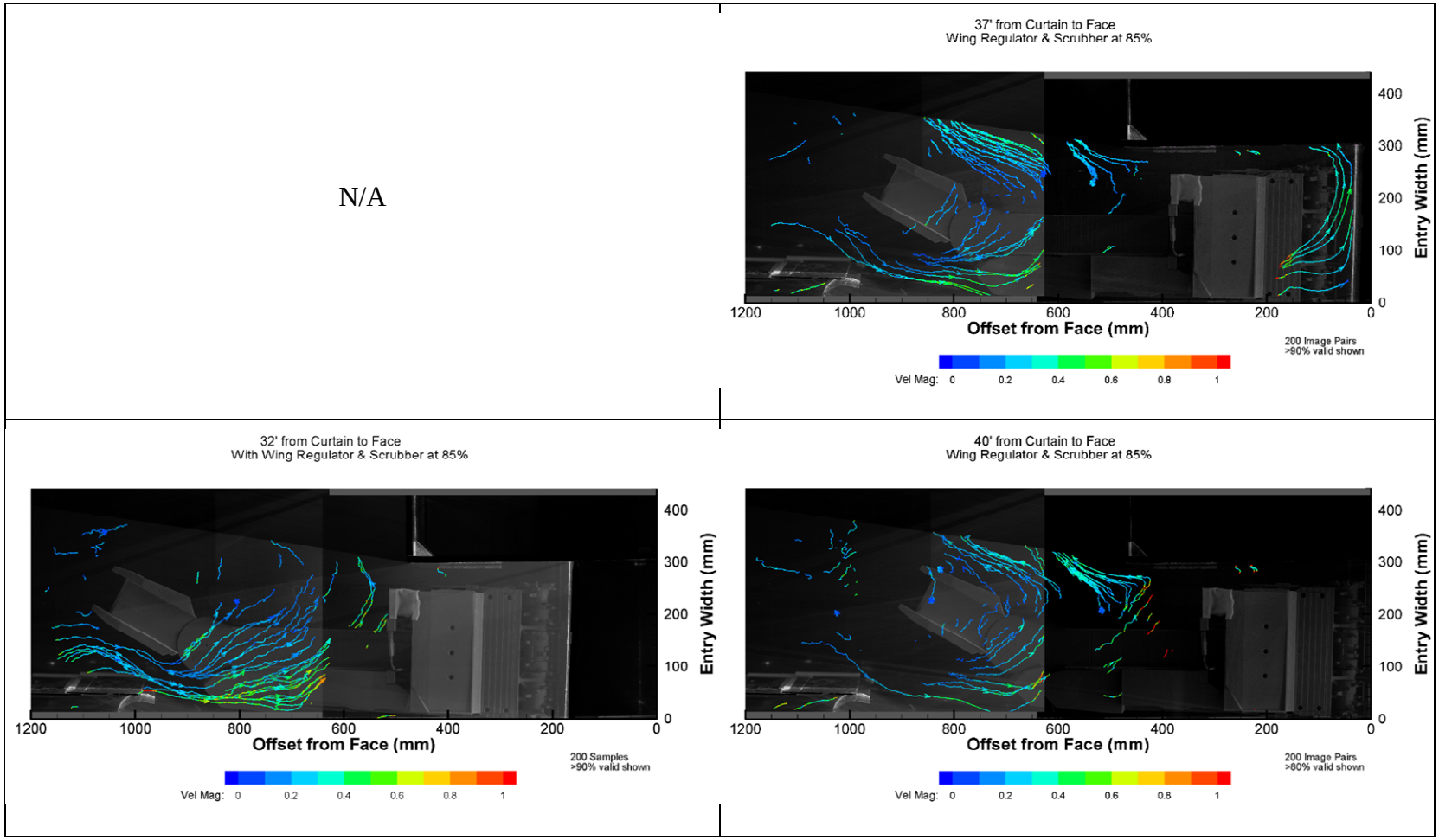

Figure 4.15 Streamline exports from Tecplot ® that illustrate the airflow changes during the progression of the box cut with the wing with the scrubber nominally set at approximately 85% of the target curtain velocity.

4.7.2 100% Scrubber Ratio

Figure 4.16 shows the average velocity calculated for three setbacks: 32, 37, and 40 feet. Immediately, it is noticeable that the PIV system was not able to properly capture particle travel in the horizontal plane. This data shows that the air consumed by the scrubber mostly overwhelms the effect caused by the wing. When the scrubber was drawing less air, the fresh air continued onto the face area. When the scrubber is consuming as much air as is entering the area, there is nowhere else to draw air from other than the stream headed towards the face. In this configuration, the scrubber is defeating the purpose of the fresh air.

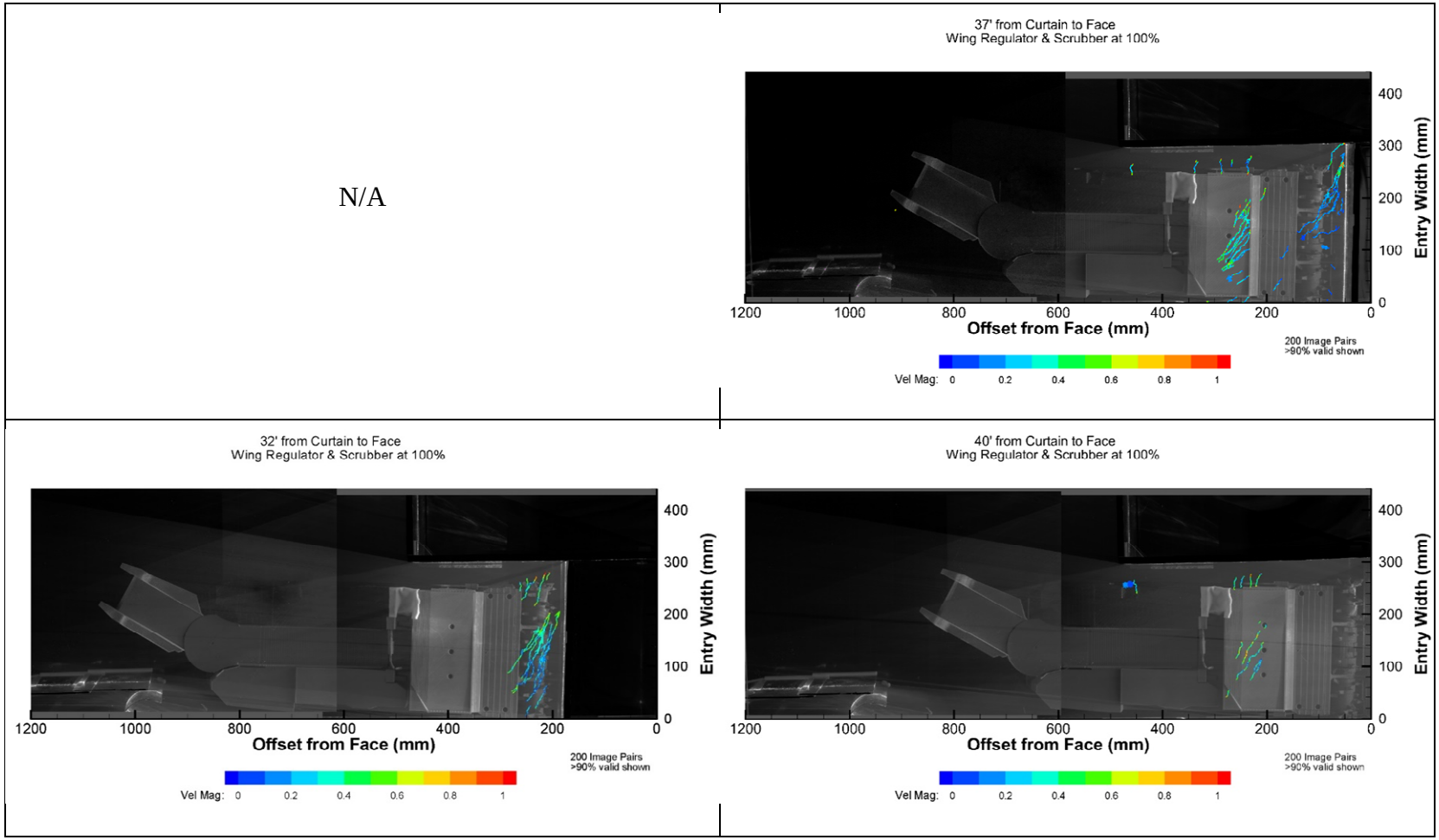

Figure 4.16 Streamline exports from Tecplot ® that illustrate the airflow changes during the progression of the box cut with the wing with the scrubber nominally set at approximately 100% of the target curtain velocity.

4.7.3 115% Scrubber Ratio

Figure 4.17 shows the average velocity calculated for three setbacks: 32, 37, and 40 feet at a scrubber to curtain ratio of 115%. Similar to the 100% scrubber-to-curtain air quantity ratio testing, the PIV system was not able to properly capture particle travel in this plane. The turbulence created in this model configuration acts in both the horizontal and vertical plan. The scrubber inlets are pulling the air down, below the plane of the PIV, while the wing is accelerating the air toward the wall.

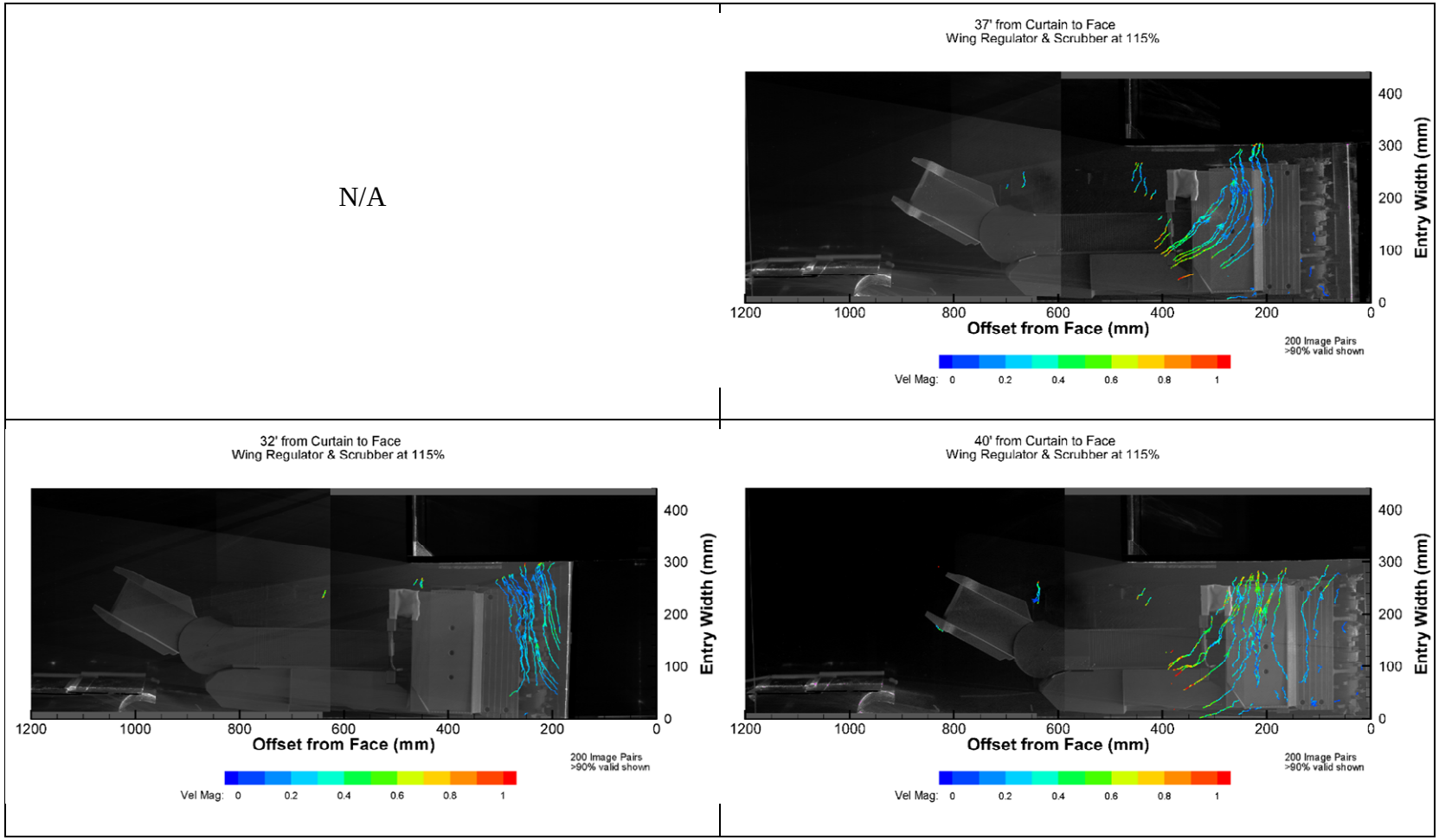

Figure 4.17 Streamline exports from Tecplot ® that illustrate the airflow changes during the progression of the box cut with the wing with the scrubber nominally set at approximately 115% of the target curtain velocity.

4.8 Fresh Air Separation

From the zones generated by Tecplot of the averaged velocities, vectors at point intervals can be extracted. For the following graphs, points have been extracted from the curtain side rib at approximately equivalent to two feet from the rib just as was done in the field and full-scale tests. The change in the velocity of the course of its travel along this profile is a characteristic of its loss of forward velocity and its separation from the wall. The velocities measured and described in the following graphs are only the x-direction velocity, or velocity travelling in parallel with the wall. The convention used in this methodology is that inby air is considered “positive” while outby traveling air is “negative”. Therefore, it is assumed that the location where the velocity is zero, is a critical location for which the air has separated from the wall. Velocity measurements (x only, y only, and velocity magnitude) were taken from the absolute 0 to absolute 1000mm of the image with 200 sample points taken for further analysis.

It is noted that, while care was taken during the setup of the test, once it began, there were changes to the curtain air velocity likely due to the movement of the miner thus changing the resistance of the flow. Due to variations in the air velocity during the PIV tests, the velocity presented has been normalized to the maximum velocity of each test set. This normalization allows the test to be compared directly. Similarly, as it was not possible to keep the model perfectly in alignment with the camera for every test, the x-axis of the graphs is in a percentage. This percentage is a calculation of the measurement point, as an absolute, compared to other measurement points as a percentage of its distance from the face relative to the curtain setback. This results in 0% representing the face and 100% representing the curtain setback. This makes comparison of different scenarios easier.

Appendix A provides an explanation of the nomenclature used in many of the graph legends.

Using the methodology just described, data was extracted for the scaled model with the miner where neither the scrubber nor wing regulator was used. Data from two similar field tests, with and without a miner, are plotted on the same graph shown in Figure 4.18.

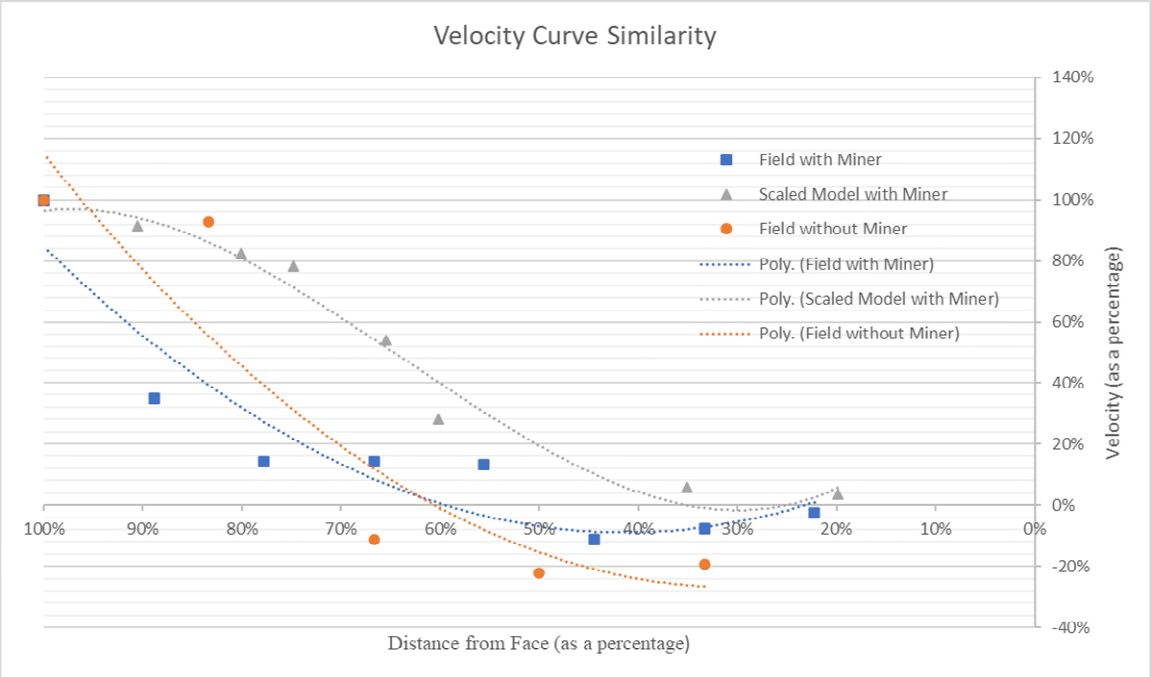

Figure 4.18 Velocity Curve Comparison for Field and Scaled Model

The model using Froude scaling produced a fresh air stream that does not leave the curtain-side wall as early as is measured in the field; however, the velocity curve shows similarity. This relationship demonstrates a shift in the curve between field and scale model.

4.8.1 Face Trajectory Profile without Scrubber or Wing

In this first test series, the progression of the miner was performed without the scrubber. Each curve in

Figure 4.19 represents a change in the setback distance as the miner progressed in its cut. The curves all follow a similar trajectory although at the beginning of the cut, there is a bump in velocity. This is due to the size and shape of the continuous miner, which fills up the entry and blocks air from flowing over the top. This further complicated the PIV readings above the miner body because it causes both upward flows and turbulence close to the plane of the laser.

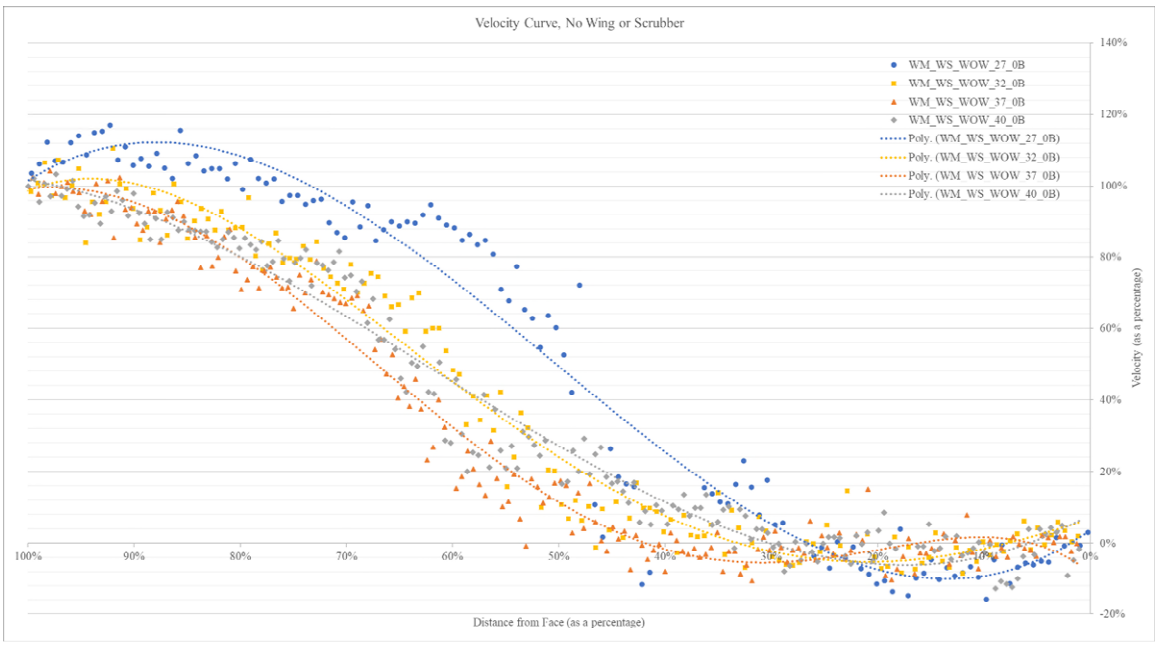

Figure 4.19 Velocity curve as the cut progressed for a continuous miner section without a scrubber or wing regulator.

The drop in velocity from the curtain to the face is represented as a percentage. Negative velocity indicates a reversal in the flow direction (i.e., outby flow). Zero velocity

on this curve corresponds with the distance whereby the air has completely changed directions. Using polynomial regression of the data points, the x-axis intersection was found (i.e., separation point of the fresh air). These values are displayed in Table 4.2.

Table 4.2 Measurements for profile curve without Scrubber or Wing Regulator

Test	Separation Point (%)	Separation Point (full-scale equivalent ft from face)
without Wing at 27 ft setback, Scrubber inactive	26.56%	*7.13*
without Wing at 32 ft setback, Scrubber inactive	*33.56%*	*10.37*
without Wing at 37 ft setback, Scrubber inactive	38.09%	*13.80*
without Wing at 40 ft setback, Scrubber inactive	*30.13%*	*11.39*

4.8.2 Face Trajectory Profile with Scrubber Only

The next graph displays the velocity change over the extracted line for tests where the scrubber was utilized. In Figure 4.23, the velocity curve is plotted for each setback for an 85% scrubber to curtain air ratio. Each setback follows a similar curve but as can be seen, the drop in velocity is steep resulting in the air losing its trajectory further from the face. The larger relative drop below the x-axis measures the size of the recirculation at the face, as illustrated in Figure 4.11.

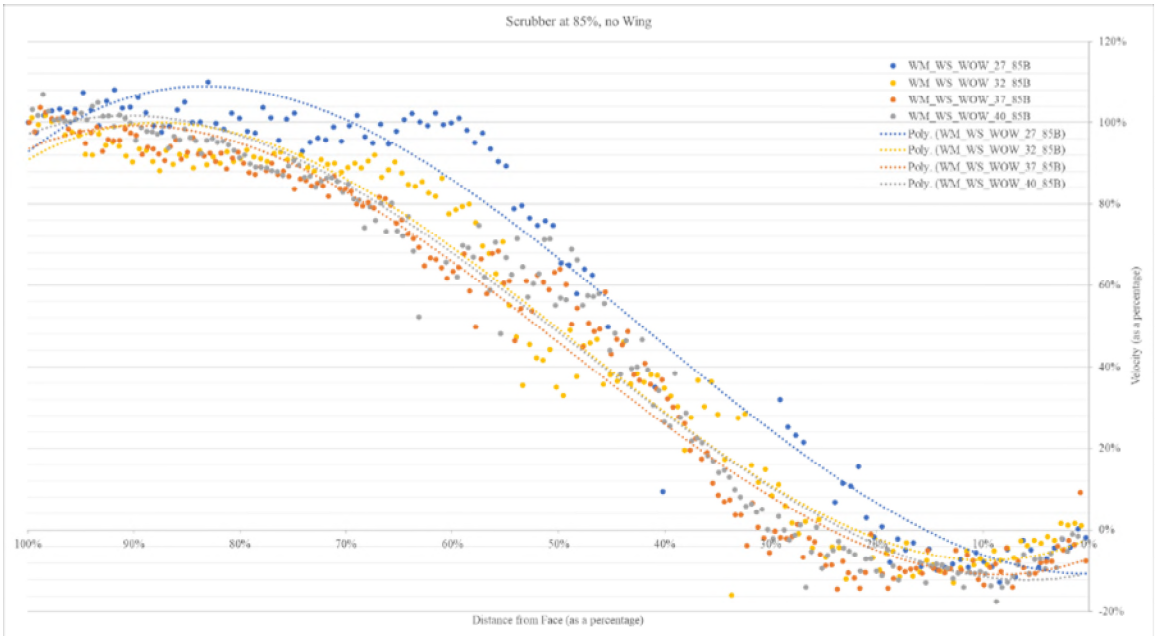

Figure 4.20 Velocity curve as the cut progressed for a continuous miner section with the scrubber set at 85% of the target curtain air.

A polynomial regression model created from the data points was used to determine the separation point, as a percentage. The results, as shown in Table 4.3, show that the air as a percentage of the total setback does not drastically change. The calculated distance is similar to the 100% scrubber setting.

Table 4.3 Measurements for profile curve with scrubber at 85% target curtain air

Test	Separation Point (%)	Separation Point (full-scale equivalent ft from face)
without Wing at 27 ft setback, Scrubber at 85%	*19.42%*	*5.2*
without Wing at 32 ft setback, Scrubber at 85%	*22.03%*	*6.87*
without Wing at 37 ft setback, Scrubber at 85%	*24.33%*	*9.03*
without Wing at 40 ft setback, Scrubber at 85%	*22.94%*	*8.84*

In Figure 4.21, each curve represents the setback distance of the curtain as the miner makes its cut with the scrubber set to 100% of the target curtain air. As in the control case, velocity falls as the curtain air makes its way towards the face area.

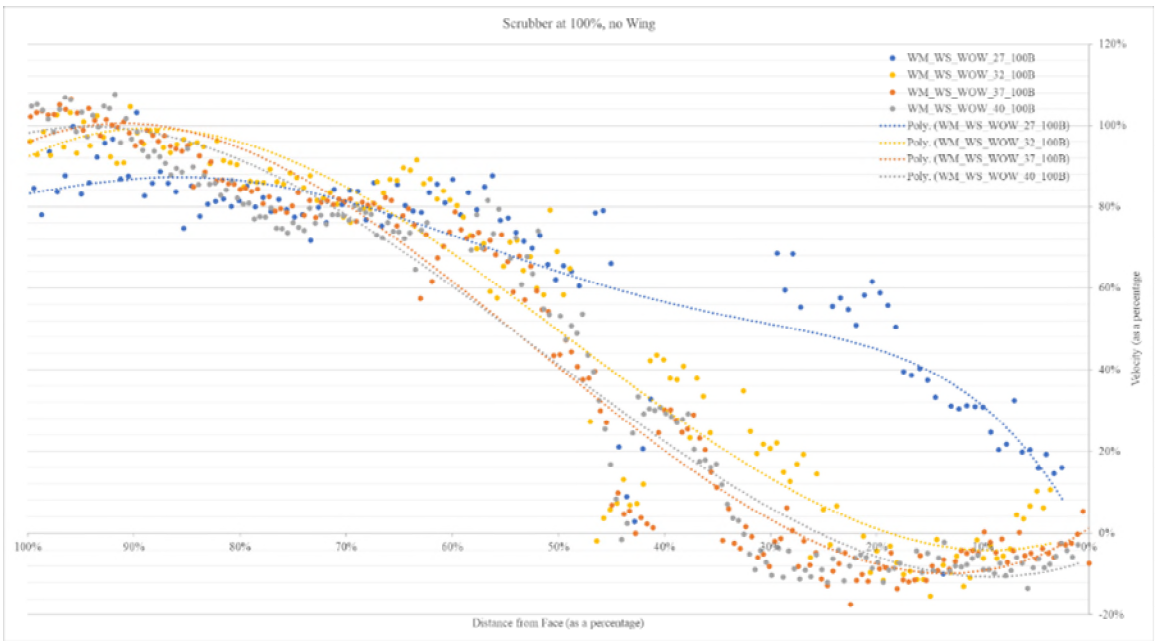

Figure 4.21 Velocity curve as the cut progressed for a continuous miner section with the scrubber set at 100% of the target curtain air.

At the beginning of the cut, the curtain air was shown to reach all the way to face. It is notable that this profile has a different trend. In this case, the velocity dropped more slowly, and a rapid drop did not occur until approximately 20% of the distance from the face to curtain. The velocity dropped at a similar rate for the remaining setback tests. The point at which each test was calculated to have changed its direction is shown below in Table 4.4.

Table 4.4 Measurements for profile Curve with Scrubber at 100% Target Curtain Air

Test	Separation Point (%)	Separation Point (full-scale equivalent ft from face)
without Wing at 27 ft setback, Scrubber at 100%	*0.69%*	*0.18*
without Wing at 32 ft setback, Scrubber at 100%	*18.84%*	*5.94*
without Wing at 37 ft setback, Scrubber at 100%	*27.63%*	*9.98*
without Wing at 40 ft setback, Scrubber at 100%	*25.46%*	*9.60*

As the scrubber air speed is increased, the fresh air was demonstrated to travel much further before changing its course. Figure 4.22 illustrates the drop in velocity along the curtain side rib as it travelled towards the face. The velocity is shown to decrease at a similar rate for all setbacks.

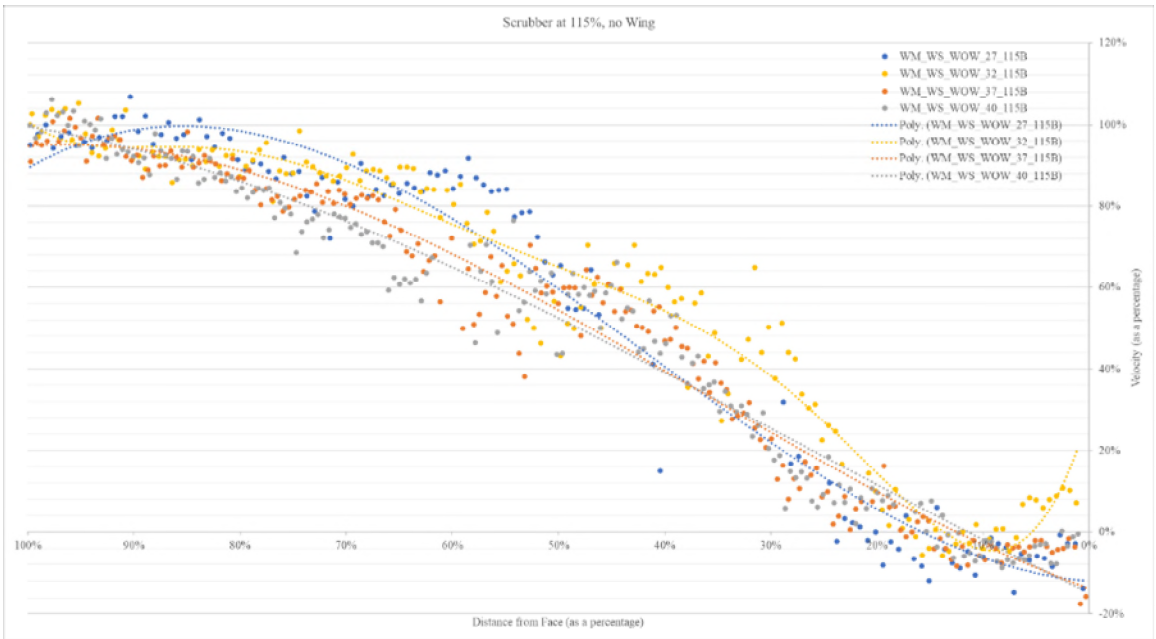

Figure 4.22 Velocity curve as the cut progressed for a continuous miner section with the scrubber set at 115% of the target curtain air.

Using polynomial regression, the x-axis intersection was calculated. This is shown in Table 4.5 When the actual measured setback is multiplied by the percentage, the

distance from the face is determined. At this scrubber ratio, the fresh air along the curtain side rib penetrated very similarly close to the face for all setbacks.

Table 4.5 Measurements for profile curve with Scrubber at 115% target curtain air

Test	Separation Point (%)	Separation Point (full-scale equivalent ft from face)
without Wing at 27 ft setback, Scrubber at 115%	*15.82%*	*4.32*
without Wing at 32 ft setback, Scrubber at 115%	*13.70%*	*4.29*
without Wing at 37 ft setback, Scrubber at 115%	*12.55%*	*4.69*
without Wing at 40 ft setback, Scrubber at 115%	*11.48%*	*4.44*

4.9 Target Setback Comparison

The following graphs are designed to help illustrate how the power settings of the scrubber change the curtain-side velocity profile. Figure 4.23 shows that the 100% Scrubber Air ratio produced the most favorable results as the velocity did not quickly drop and the fresh air made it all the way to face area.

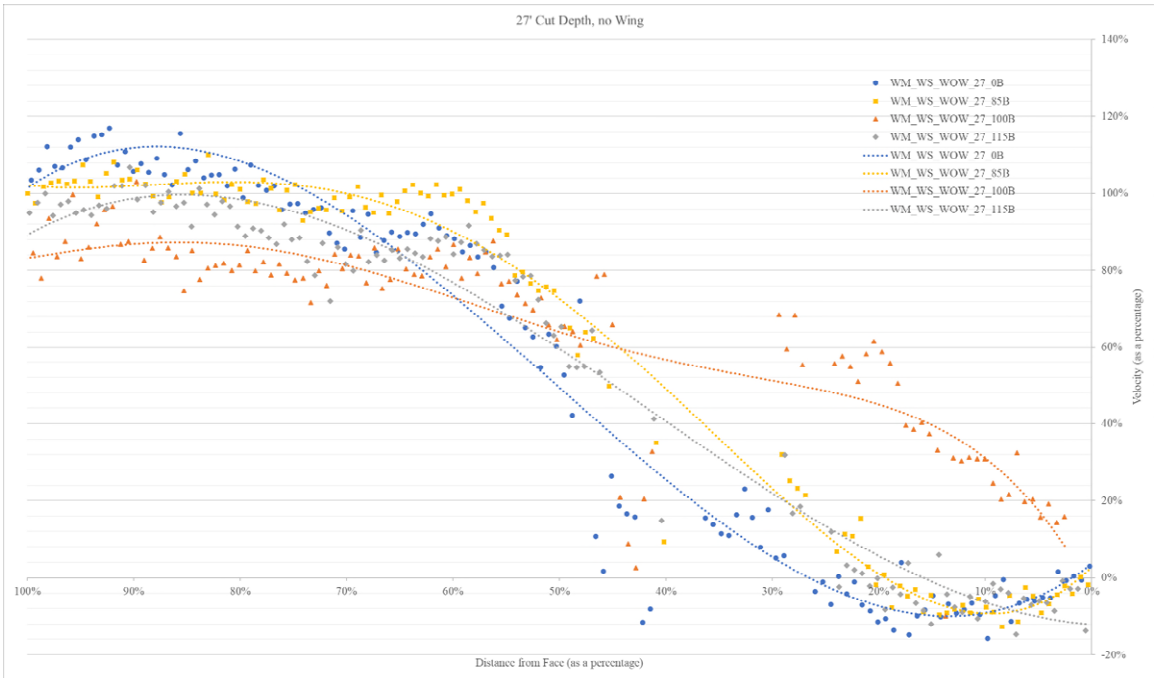

Figure 4.23 Velocity plots at each scrubber setting for the 27-ft setback

For Figures 4.24, 4.25, and 4.26 , the velocity plots follow very similar paths respectively. For these plots, the 115% scrubber ratio is seen with a profile furthest to the right of the graph which indicates that this setting promotes the fresh air to stay along the curtain-side rib the longest and at the highest velocity relative to the supplied curtain air. Without the assistance of the scrubber, the fresh air does not make it as far and the deep curve below the x-axis shows the area of recirculation.

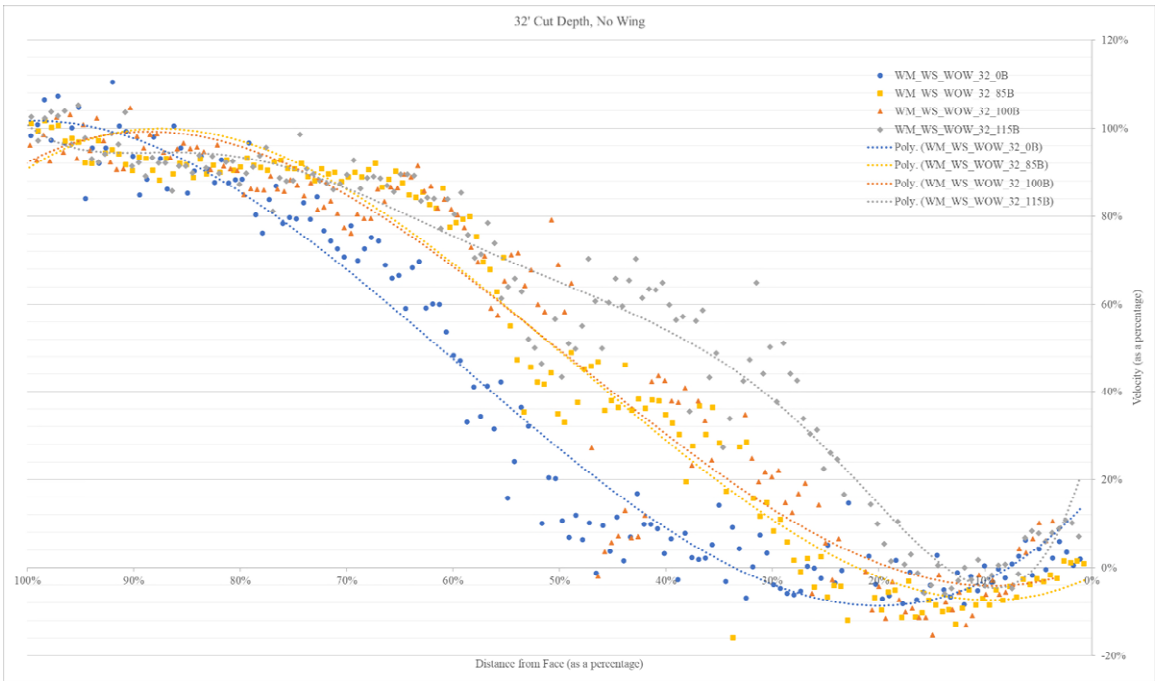

Figure 4.24 Velocity plots at each scrubber settings at the 32-ft setback

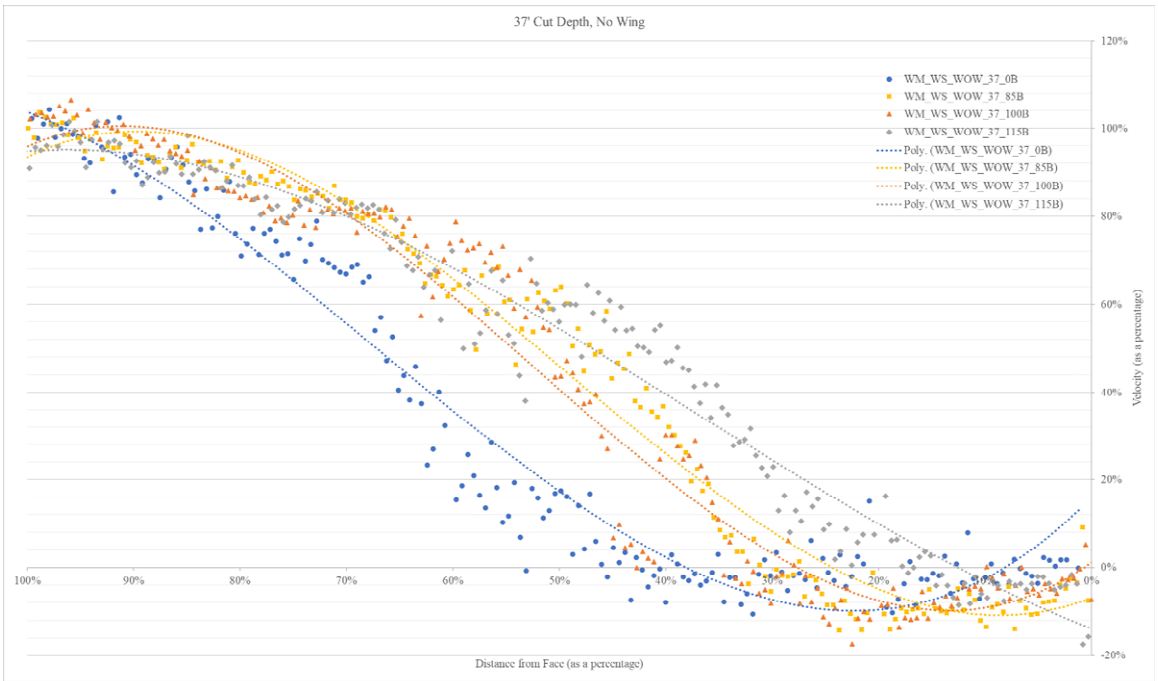

Figure 4.25 Velocity plots at each scrubber setting at the 37-ft setback

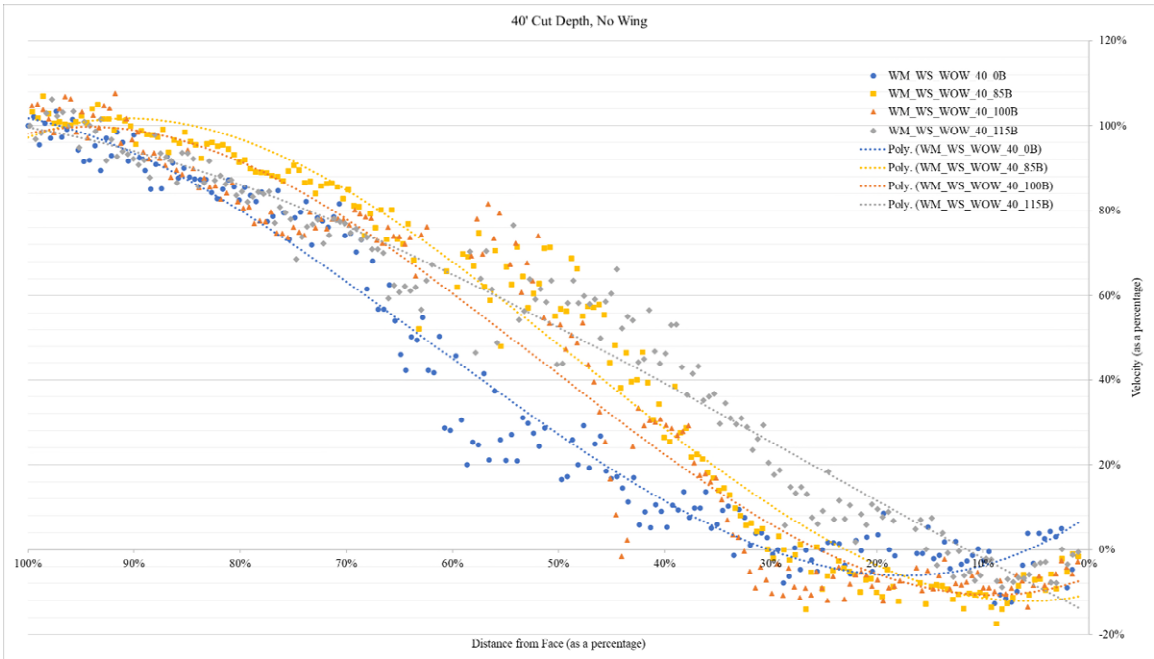

Figure 4.26 Velocity plot at each scrubber setting at the 40-ft setback

These graphs show that the dust scrubbers must pull fresh air toward the face, which is maximum when the face, scrubber inlet and curtain are closest to each other, but is greatly diminished as the depth increases. As shown in the velocity vector figures, the scrubber is itself consuming the air from the curtain at the one to one or higher ratio. This does pull it toward the face, but not where the fresh air is needed.

4.10 Overview of Results

The model, a near replica of the dust gallery, has a moveable face which allows for different cut depths to be achieved. The line brattice is positioned 40” from the front acrylic piece and 4” from the rib. This was consistent for all experiments shown in this dissertation. Only the face piece is allowed to move with the pulling of the floor slider which is marked for each setback position: 27”, 32”, and 37”. The 40” setback is the position where the face cannot move any further forward and is pressed firmly against the front acrylic.

Small inaccuracies in the face position are caused by being moved by hand as well as shifts in the face from perpendicular. Therefore, the actual setback distance is calculated for each test using the image captures. In Tecplot, the pixels from face to curtain is measured and then converted to a distance using the image calibration data.

The velocity is set at the beginning of the test, but it did not remain constant over the entirety of the experimental run. The established procedure did not allow for the glass top to be moved during the run and so the velocity could not be measured again with the hot wire anemometer probe and adjusted. Instead, the PIV system was used to measure the average fresh air velocity post run to correct value for each setback. The scrubber ratio was updated to reflect the changes in fresh air velocity. The scrubber's airflow itself remained consistent throughout the tests and was monitored remotely.

The separation point as a distance was determined by multiplying the corrected setback value by the percentage determined using the regression models previously shown.

All experiments were set up to target a reduced scale velocity of 0.52 m/s to simulate a 10,000 CFM curtain air quantity. From the individual PIV measurements, the actual velocity at the curtain in the laser plane was measured as was actual setback value from images. These values are summarized in Table 4.6.

Table 4.6 Summary of measured PIV results

Test Description	Setback (ft)	Curtain Velocity (m/s)	Corrected Scrubber Ratio	Separation Point (%)	Separation Point (ft)
without Wing at 27 ft setback, Scrubber inactive	26.86	0.52	-	26.56%	7.13
without Wing at 27 ft setback, Scrubber at 85% Ratio	26.80	0.43	105%	19.42%	5.20
without Wing at 27 ft setback, Scrubber at 100% Ratio	26.55	0.33	158%	0.69%	0.18
without Wing at 27 ft setback, Scrubber at 115% Ratio	27.32	0.41	149%	15.82%	4.32
without Wing at 32 ft setback, Scrubber inactive	30.91	0.44	-	33.56%	10.37
without Wing at 32 ft setback, Scrubber at 85% Ratio	31.20	0.45	99%	22.03%	6.87
without Wing at 32 ft setback, Scrubber at 100% Ratio	31.50	0.42	124%	18.84%	5.94
without Wing at 32 ft setback, Scrubber at 115% Ratio	31.35	0.39	154%	13.70%	4.30
without Wing at 37 ft setback, Scrubber inactive	36.22	0.46	-	38.09%	13.80
without Wing at 37 ft setback, Scrubber at 85% Ratio	37.15	0.49	91%	24.33%	9.04
without Wing at 37 ft setback, Scrubber at 100% Ratio	36.11	0.54	97%	27.63%	9.98
without Wing at 37 ft setback, Scrubber at 115% Ratio	37.40	0.46	131%	12.55%	4.69
without Wing at 40 ft setback, Scrubber inactive	37.80	0.38	-	30.13%	11.39
without Wing at 40 ft setback, Scrubber at 85% Ratio	38.54	0.50	89%	22.94%	8.84
without Wing at 40 ft setback, Scrubber at 100% Ratio	37.73	0.55	95%	25.46%	9.60
without Wing at 40 ft setback, Scrubber at 115% Ratio	38.66	0.46	130%	11.48%	4.44

CHAPTER 5. MAJOR CONCLUSIONS AND FUTURE WORK

Mine ventilation provides predictable and sufficient fresh air to the underground mine workings to support the health of workers, dilute noxious gases, and remove dust. The ventilation system requires a significant amount of energy, which should be used efficiently where it is needed, especially at freshly broken rock along the working face. This dissertation discusses a methodology for studying face ventilation using a reduced-scale model and particle image velocimetry (PIV) to assist the practicing engineer to optimize the ventilation system. Conclusions about the different components of this study are discussed in the following sections.

5.1 Practicality of Froude Scaling

Reynold's scaling, which equates the forces of viscosity between full- and reduced-scale, is generally the default scaling law that has been applied to modelling continuous-miner-section face ventilation in previous studies, e.g., as discussed in Chapter 2. Modelling using Reynolds number scaling, given in Equation 3.6, with the full-scale flow regimes found in typical mining operation leads to unrealistic model conditions. For example, to model the airflow quantity of 10,000 CFM through the 1/12th scale (i.e., $\frac{l}{l'} = 12$) dust scrubber, where the air velocity is approximately 4,100 fpm, the scaled velocity would be 49,200 fpm through an approximately two in^2 opening. Practical equipment was determined to be unable to achieve this value.

Using Froude number, scaling results in a much smaller and achievable velocity, which can be reasonably obtained with readily available equipment. The comparison in Figure 4.18 demonstrates that the Froude scaling law produces scaled model results that

closely follow the airflow pattern observed in the full-scale model. For the modeler, both approaches should be calculated, and the flow regimes evaluated. If the Reynolds scaling produced regimes that are unachievable, the flow pattern may be developed using Froude number scaling and careful model construction with validation.

5.2 Particle Image Velocimetry for Face Ventilation Study

Face airflow data is difficult to collect at full-scale, especially at an operating mine. It can be either impractical or too intrusive to set up a high number of sample points needed to fully characterize airflow. As discussed in Section 3.6, PIV testing offers an alternative method of collecting high resolution air velocity data over the entire area of a plane in reduced-scale models. Also, the PIV system can capture instantaneous velocity measurements for the entire field multiple times per session.

However, as was demonstrated, especially in the wing regulator and scrubber combined tests (Sections 4.7), turbulence made PIV measurements unreliable for measuring flow. As shown, seed particles are only introduced at the intake. Eddy zones may have affected the particle density set at the beginning of the experiment. More critically, particles that are moving perpendicular to the plane of the laser light sheet prevent the system from tracking displacement. Decreasing the ΔT value because the particle's trajectory is not contained solely in the horizontal plane does not improve the quality. While relatively small vertical movements can be handled by taking a large sample size (i.e., number of captures), the methodology used was unable to capture the entire air pattern.

5.3 Practicality of Reduced-Scale modeling

In the case of mine face ventilation and this study, models must be based on real world measurements. From the general field testing, described in Section 4.1, the general airflow patterns of a typical mine face were measured. By taking several mine samples, variations in those patterns and airflow regimes were determined. Initial full-scale model flow did not match the field testing, highlighting the importance of other factors than the typical flow values (i.e., quantity, velocity, and pressure) most notably turbulence intensity, discussed below.

Reduced-scale models complement a full-scale model. For example, when investigating the turbulence intensity association with flow separation in the full-scale model, the baffles could be trialed in the reduced scale model before investing at full-scale.

The operating conditions, e.g., cut depth, setback distance, and air quantity, can be more easily changed at reduced scale, allowing for the development of a deeper understanding of the flow characteristics than could otherwise be achieved with little incremental expense in time and materials. Majority of the time and expense is in the initial build of the model and equipment.

5.4 Turbulence Intensity

The turbulence intensity (TI) of the curtain airflow was an important factor for making the airflow patterns similar. As discussed in Section 4.2, there are challenges to increasing the TI. In the mine, the roughness, turns, and length, which can be miles underground, of the airways naturally increase the TI values to 8% or greater. In a full-scale or reduced scale model, the intake air is generally from a large, low turbulent area.

Baffles were determined to be a critical structure for matching the flow pattern in our models to the field testing.

5.5 Velocity Curve Approach

The approach presented in Chapter 4 of this dissertation is demonstrated as a method for evaluating the inby flow of fresh air from the curtain towards the face. The further air travels toward the face, the more that would be delivered to the point it is needed. Normalizing the data and using the percentage of tight side air velocity allows for the comparison of profiles from various line brattice setback distances and air quantities to predict the separation point. This could be used for any mine face configuration where the ventilation delivery system must be setback from the cutting or drilling operation.

5.6 Effect of Scrubber Ratio on the Separation Point

As shown in Table 4.6, scenarios where the scrubber is inactive, the separation point is further away from the face. The scrubber can act as a vacuum, especially in a deep box cut, causing the curtain air velocity to increase. This increase is not sufficient in cases where the scrubber is at or above 100% exacerbating the recirculation as seen in image such as Figure 4.12.

The relationship between the scrubber-to-curtain air quantity ratio and distance to the air separation point is illustrated in Figure 5.1. This plot shows that, as the scrubber-to-curtain air ratio increases, the separation point distance decreases; however, the fresh air is likely being drawn directly into the inlets of the scrubber and is not ventilating the cutting point, where it is most necessary.

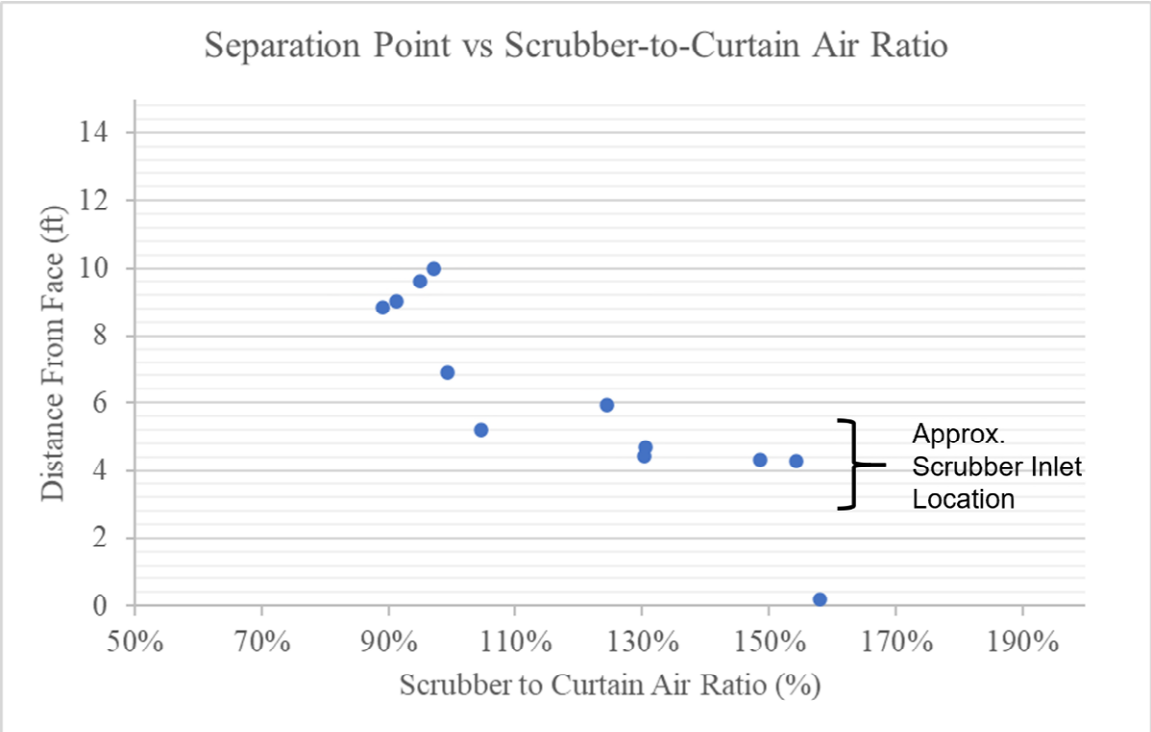

Figure 5.1 Separation point, in full-scale equivalent, versus the corrected scrubber flow ratio, as percentage of curtain air.

5.7 Future Considerations

The following items have been identified as avenues for future work:

1. The laser and camera setup could be rearranged such that the laser sheet is vertical and the camera views through a rib wall to measure the velocity in the vertical plane. This should produce similar x-direction air velocity as used in the methodology applied here but might account for the swirling and vertical air movements.
2. To better measure the changes in the overall curtain air flow, a small air speed sensor could be developed and implemented so that changes in this quantity can be monitored throughout the continuous miner models movements.
3. The reduced-scale model apparatus is capable of image capture while the miner is moving, both advancing the face and the cutting drum rotating. However, there are difficulties in the PIV system for interpreting the data while the reduced scale model is moving. Developing a more complex method for coordinating movement with image capture may yield interesting results and allow work on items like water sprays.
4. This research focused on the more difficult ventilation scenario, the box cut. The slab cut could be investigated in a similar manner.

APPENDIX A. TESTING ABBREVIATION

Testing abbreviations were developed for naming experiments in Insight 4G.

Key:

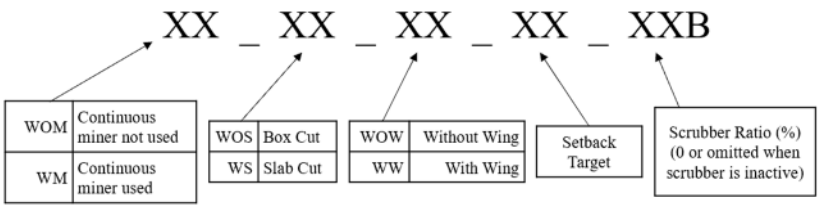

Table A-1 Explanation of Test Abbreviations

Abbreviation	Explanation
WM_WS_WOW_27	Box Cut test with CM Model, without Wing at 27 ft setback, Scrubber inactive
WM_WS_WOW_27_115B	Box Cut test with CM Model, without Wing at 27 ft setback, Scrubber at 115% Ratio
WM_WS_WOW_27_85B	Box Cut test with CM Model, without Wing at 27 ft setback, Scrubber at 85% Ratio
WM_WS_WOW_32	Box Cut test with CM Model, without Wing at 32 ft setback, Scrubber inactive
WM_WS_WOW_32_100B	Box Cut test with CM Model, without Wing at 32 ft setback, Scrubber at 100% Ratio
WM_WS_WOW_32_115B	Box Cut test with CM Model, without Wing at 32 ft setback Scrubber at 115% Ratio
WM_WS_WOW_32_85B	Box Cut test with CM Model, without Wing at 32 ft setback, Scrubber at 85% Ratio
WM_WS_WOW_37	Box Cut test with CM Model, without Wing at 37 ft setback, Scrubber inactive
WM_WS_WOW_37_100B	Box Cut test with CM Model, without Wing at 37 ft setback, Scrubber at 100% Ratio
WM_WS_WOW_37_115B	Box Cut test with CM Model, without Wing at 37 ft setback Scrubber at 115% Ratio
WM_WS_WOW_37_85B	Box Cut test with CM Model, without Wing at 37 ft setback, Scrubber at 85% Ratio
WM_WS_WOW_40	Box Cut test with CM Model, without Wing at 40 ft setback, Scrubber inactive
WM_WS_WOW_40_100B	Box Cut test with CM Model, without Wing at 40 ft setback, Scrubber at 100% Ratio
WM_WS_WOW_40_115B	Box Cut test with CM Model, without Wing at 40 ft setback Scrubber at 115% Ratio
WM_WS_WOW_40_85B	Box Cut test with CM Model, without Wing at 40 ft setback, Scrubber at 85% Ratio

Table A-1 Explanation of Test Abbreviations (continued)

Abbreviation	Explanation
WM_WS_WW_27	Box Cut test with CM Model, with Wing at 27 ft setback, Scrubber inactive
WM_WS_WW_27_115B	Box Cut test with CM Model, with Wing at 27 ft setback, Scrubber at 115% Ratio
WM_WS_WW_27_85B	Box Cut test with CM Model, with Wing at 27 ft setback, Scrubber at 85% Ratio
WM_WS_WW_32	Box Cut test with CM Model, with Wing at 32 ft setback, Scrubber inactive
WM_WS_WW_32_100B	Box Cut test with CM Model, with Wing at 32 ft setback, Scrubber at 100% Ratio
WM_WS_WW_32_115B	Box Cut test with CM Model, with Wing at 32 ft setback Scrubber at 115% Ratio
WM_WS_WW_32_85B	Box Cut test with CM Model, with Wing at 32 ft setback, Scrubber at 85% Ratio
WM_WS_WW_37	Box Cut test with CM Model, with Wing at 37 ft setback, Scrubber inactive
WM_WS_WW_37_100B	Box Cut test with CM Model, with Wing at 37 ft setback, Scrubber at 100% Ratio
WM_WS_WW_37_115B	Box Cut test with CM Model, with Wing at 37 ft setback Scrubber at 115% Ratio
WM_WS_WW_37_85B	Box Cut test with CM Model, with Wing at 37 ft setback, Scrubber at 85% Ratio
WM_WS_WW_40	Box Cut test with CM Model, with Wing at 40 ft setback, Scrubber inactive
WM_WS_WW_40_100B	Box Cut test with CM Model, with Wing at 40 ft setback, Scrubber at 100% Ratio
WM_WS_WW_40_115B	Box Cut test with CM Model, with Wing at 40 ft setback Scrubber at 115% Ratio
WM_WS_WW_40_85B	Box Cut test with CM Model, with Wing at 40 ft setback, Scrubber at 85% Ratio

REFERENCES

ABC Industries. (2021). Brattice/Curtains. Retrieved from https://www.abc-industries.net/products/brattice-curtains-flypads

Bise, C. J. (1986). Ventilation. In *MINING ENGINEERING ANALYSIS* (p. 23). Littleton: SME.

Colinet, J. F., McClelland, J. J., Erhard, L. A., & Jankowski, R. A. (1990). *RI 9313: Laboratory Evaluation of Quartz Dust Capture of Irrigated-Filter Collection Systems for Continuous Miners*. Spokane, WA.

Colinet, J. F., Reed, W., & Potts, J. D. (2013). Impact on Respirable Dust Levels When Operating a Flooded-bed Scrubber in 20-foot Cuts. In *DHHS (Niosh) Publication 2014-105, Ri 9693*. Pittsburgh, PA.

Colinet, J. F., Rider, J. P., Listak, J. M., Organiscak, J. A., & Wolfe, A. L. (2010). Best Practices for Dust Control in Coal Mining. In *IC 9517 Information Circular: Best Practices for Dust Control in Coal Mining* (Vol. 01).

Goodman, G. V. R., & Taylor, C. D. (1993). Chapter 4: A technique for evaluating scrubber recirculation during deep cut mining. *Proceedings of the 6th US Mine Ventilation Symposium*, 19–24. Littleton, CO: Society of Mining, Metallurgy, and Exploration, Inc.

Goodman, G. V. R., Taylor, C. D., Colinet, J. F., & Thimons, E. D. (2000). NIOSH Research for Controlling Respirable Dust and Methane Gas on Continuous Miner Faces. *Proceedings of the 12th International Conference on Coal Research, Sandton, Republic of South Africa, September 12-15, 2000*, 151–154. Johannesburg, South Africa: South Africa Institute of Mining and Metallurgy.

Hall, N. B., Blackley, D. J., Halldin, C. N., & Laney, A. S. (2019). Current Review of Pneumoconiosis Among US Coal Miners. *Current Environmental Health Reports*, *6*(3), 137–147. https://doi.org/10.1007/s40572-019-00237-5

Honkanen, M., & Nobach, H. (2005). Background extraction from double-frame PIV images. *Experiments in Fluids*, *38*(3), 348–362. https://doi.org/10.1007/s00348-004-0916-x

Kiger, K. (2010). Introduction of Particle Image Velocimetry. *Burgers Program For Fluid Dynamics*, 57. Retrieved from https://www2.cscamm.umd.edu/programs/trb10/presentations/PIV.pdf%0Ahttp://www2.cscamm.umd.edu/programs/trb10/presentations/PIV.pdfm

Kumar, A. R., Henderson, K. M., & Schafrik, S. (2021). *Scale Modeling, PIV, and Large Eddy Simulations in a Deep Cut Blowing Type Continuous Mining Section*. Lexington, KY.

McPherson, M. J. (1993a). Background to Subsurface Ventilation. In *Subsurface Ventilation Engineering* (pp. 1–8). Mine Ventilation Services.

McPherson, M. J. (1993b). *Subsurface Ventilation and Environmental Engineering* (Vol. 1). https://doi.org/10.10017/978-94-011-1550-6

NIOSH. (2008). *Work-related lung disease surveillance report 2007, Volume 1 DHHS (NIOSH) Publication No. 2008-143a*. Cincinnati, OH.

Oswald, N., Prosser, B., & Ruckman, R. (2008). Measured values of coal mine stopping resistance. *Coal Age*, *113*(12), 40–43.

Petrov, T., Wala, A. M., & Huang, G. (2013). Parametric study of airflow separation phenomenon at face area during deep cut continuous mining. *Mining Technology*, *122*(4), 208–2014. Retrieved from Academic Search Complete, EBSCOhost (accessed November 15, 2016

Potts, J. D., Reed, W., & Colinet, J. F. (2011). *RI 9680 Evaluation of face dust concentrations at mines using deep-cutting practices*. Pittsburgh, PA.

Reed, W., & Taylor, C. (2007). Factors affecting the developing of mine face ventilation systems in the 20th century. *National Institute for Occupational Safety and Health*. Retrieved from http://www.cdc.gov/niosh/mining/UserFiles/works/pdfs/fatdo.pdf

Schafrik, S. (2019). *Alpha Foundation for the Improvement of Mine Safety and Health Final Technical Report AFC215 – 15 Improved Face Ventilation for Extended-Cut Continuous Mining Using a Wing Regulator and Scrubber Control System*.

Schultz, M. J., & Fields, K. G. (1999). DUST CONTROL CONSIDERATIONS FOR DEEP CUT MINING SECTIONS. In *Preprint 99-163*. Littleton, CO: SME.

Stricklin, K. G. (2012). *Reissue of I10-V-09- Procedures for Evaluation of Requests to Make Extended Cuts with Remote Controlled Continuous Machines*.

Taylor, C. D., Chilton, J. E., Hall, E., & Timko, R. J. (2006). Effect of Scrubber Operation on Airflow and Methane Patterns at the Mining Face. *Proceedings of the 11th US/North American Mine Ventilation Symposium*, 393–400. Retrieved from https://www.cdc.gov/niosh/mining/UserFiles/works/pdfs/eosoo.pdf

Taylor, C. D., Rider, J. P., & Thimons, E. D. (1997). IMPACT OF UNBALANCED INTAKE AND SCRUBBER FLOWS ON FACE METHANE CONCENTRATIONS. *6th International Mine Ventilation Congress Proceedings*. Retrieved from https://www.cdc.gov/niosh/mining/UserFiles/works/pdfs/eosoo.pdf

Thimons, E. D., Taylor, C. D., & Zimmer, J. A. (1999). Ventilating the Box Cut of a Two-Pass 40-ft Extended Cut. *Journal of the Mine Ventilation Society of South Africa*, *Jul 52*(3), 108–115. Retrieved from http://www.cdc.gov/niosh/mining/works/coversheet1090.html

Troolin, D., Hortensius, R., & Lai, W. T. (2020). PIV Leak Assessment of N95 Respirators. Retrieved from tsi.com website: https://tsi.com/resources/piv-leak-assessment-of-n95-respirators/

TSI. (2013). How Frame Straddling Works. Retrieved from tsi.com website: www.tsi.com/getmedia/80f5dbd-7268-4cc8-a414-cfc6866f91d0/How Frame-Straddling Works__1

TSI Inc. (2014). *Insight 4G Global Image, Acquisition, Analysis, & Display Software*. (June).

US Department of Labor. *30 CFR 70.101, Part 70-Mandary Health Standards - Underground Coal Mines - Title 30 - Code of Federal Regulations.* , (2016).

Wala, A., Jacob, J., Brown, J., & Huang, G. (2003). New approaches to mine-face ventilation. *Mining Engineering*, *55*(3), 25–30.

Wala, A. M., Jacob, J. D., Huang, G., Brown, J., & Rangubhotla, L. (2004). How scrubbers help ventilate the face during deep cut mining with a blowing curtain. *Proceedings of the 10th US/North American Mine Ventilation Symposium*, 306–314. Retrieved from http://www.cdc.gov/niosh/nioshtic-2/20026737.html

Wala, A. M., Vytla, S., Taylor, C. D., & Huang, G. (2007). Mine Face Ventilation: A Comparison of CFD Results against Benchmark Experiments for the CFD Code Validation. *Mining Engineering*, *59*(10), 49–55.

WHO. (1999). Definitions and Concepts. In *Hazard Prevention and Control in the Work Environment: Airborn Dust* (pp. 1–96). https://doi.org/10.23943/princeton/9780691143620.003.0002

Williams, M. A. (2005). UNDERGROUND COAL MINING : FACTORS , COST , AND TIME CONSIDERATIONS. *NCCI : The Coal Institute Fall Meeting*. Retrieved from http://www.thecoalinstitute.org/ckfinder/userfiles/files/Fall_Skelly_Loy.pdf

Wirch, S., & Jankowski, R. A. (1991). Shearer-Mounted Scrubbers, are They Viable and Cost Effective. *Proceedings of the 7th US Mine Ventilation Symposium*, 319–325.

VITA

Kayla Mayfield Henderson, PE
Mount Sterling, Ky

Education

MS in Mining Engineering, 2015

University of Kentucky.
Project Report Title: Automation of Laboratory Mine Ventilation Fan
Advisor: Dr. Thomas Novak, Professor of Mining Engineering

BS In Mining Engineering, 2012
University of Kentucky.

Work Experience

Mining Engineer June 2018 -Present
Groff Engineering & Consulting LLC
Mt. Sterling, Ky

Safety Intern Summer 2014
Patriot Coal
Charleston, Wv

Graduate Engineer May 2012 – April 2013
Minova USA
Georgetown, KY

Mining Engineering Intern Summer 2011
International Coal Group
Hazard, KY

Mining Engineering Intern Summer 2010
Massey Energy
Sidney, KY

Publications

Kumar, A.R., Henderson, K. M., & Schafrik, S.J. (2021). Detached Eddy Simulations of Airflows inside a Reduced Scale Model of an Entry in a Continuous Mining Section. Proceedings of 18th North American Mine Ventilation Symposium, Virtual Event.

Novak, T., & Mayfield, K. N. (2017). Development of an automation laboratory and courses for mining engineering education. SME Preprint No. 17-039. Englewood, CO: SME.

Conference Presentations

Henderson, K.M. (2020) Reduced-Scale Modeling of Machine Mounted Scrubber, Presented at the KY PEM Seminar. September 11, 2020. Lexington, KY

Mayfield, K.N., Novak, T., & Schafrik, S.J. (2019) Study of Airflow Patterns during the advancement of the face in Extended-Cuts using Particle Image Velocimetry. SME 2019 Annual Conference and Expo, Denver, CO, February 24-27.

Mayfield, K.N. (2018). Scaled-Model Testing for the Effect of Turbulent Intensity on Continuous Miner Face Ventilation. SME 2018 Annual Conference and Expo, Minneapolis, MN, February 25-28.

Mayfield, K.N., Novak, T., and Wedding, W.C. (2016, February). Automation of a Mine Ventilation Laboratory Fan. Presented at the 2016 SME Annual Conference & Expo, Phoenix, AZ.

Poster Presentations

Mayfield, K.N., Schafrik, S.J., & Novak, T. (2018). Analysis of face ventilation during extended cut sequence using particle image velocimetry. Poster presented at the SME 2018 Annual Conference and Expo, Minneapolis, MN, February 25-28.

Mayfield, K.N., Schafrik, S.J., Novak, T., & Sottile, J. (2018). Study for improved capture efficiency of machine-mounted dust scrubbers in coal mining applications. Poster presented at the Southeastern Regional ERC Symposium, Savannah, GA, April 3-4.

Teaching Experience

Graduate Teaching Assistant
University of Kentucky
Mine Ventilation (Lab)

Memberships / Affiliations

Society of Mining, Metallurgy, and Exploration